HARVARD UNIVERSITY
Graduate School of Arts and Sciences

DISSERTATION ACCEPTANCE CERTIFICATE

The undersigned, appointed by the

Division of Medical Sciences

in the subject of Human Biology and Translational Medicine

have examined a dissertation entitled

Glucose Metabolism in Cancer-Associated Fibroblasts

presented by Annie Phuong Vo

candidate for the degree of Doctor of Philosophy and hereby certify that it is worthy of acceptance.

Signature: _____

Typed Name: Dr. Bruce Zetter

Signature: _____

Typed Name: Dr. Zoltan Arany

Signature: _____

Typed Name: Dr. David Housman

_____

Dr. David Van Vactor, Program Head

Date: April 04, 2013

_____

Dr. David Lopes Cardozo, Director of Graduate Studies

Glucose Metabolism in Cancer-Associated Fibroblasts

A dissertation presented

by

Annie Phuong Vo

to

The Division of Medical Sciences

In partial fulfillment of the requirements

for the degree of

Doctor of Philosophy

in the subject of

Human Biology and Translational Medicine

Harvard University

Cambridge, Massachusetts

April, 2013

ProQuest LLC.
789 East Eisenhower Parkway
P.O. Box 1346
Ann Arbor, MI 48106 - 1346

Dissertation Advisor: Raghu Kalluri Annie Phuong Vo

Glucose Metabolism in Cancer-Associated Fibroblasts

ABSTRACT

Under normal conditions, non-transformed cells rely on glycolysis followed by oxidative phosphorylation to generate ATPs. When oxygen is scarce or when cells are actively proliferating, cellular ATPs come mainly from glycolysis. Pyruvate is converted into lactate to allow glycolysis to continue. Interestingly, cancer cells have adapted to favor lactate production even at normal oxygen tensions, exhibiting a metabolic shift known as the Warburg effect. However, the metabolic state of other cellular constituents within the tumor remains mostly unknown.

Cancer-associated fibroblasts (CAFs) are the most abundant stromal cells. They aid tumor growth and metastasis by providing growth factors, cytokine, ECM remodeling proteins and interacting with other tumor stromal cells. Here I show that the Warburg effect also operates in stromal fibroblasts of the tumor microenvironment. Using mass spectrometry, genetic mouse models, gene expression and methylation studies, I demonstrate that CAFs from human and mouse mammary tumors exhibit hyperactive glycolysis and a metabolic shift towards lactate production. Furthermore, this phenotype may be sustained through epigenetic modifications of endogenous hypoxia-inducible factor 1α, key regulatory enzymes fructose-bisphosphatase 1 and pyruvate kinase M2. Depletion of stromal fibroblasts or suppression of lactate production specifically in these cells alters the metabolic profile of not only the tumors but also the cancer cells and results in impeded tumor growth.

These results collectively suggest that tumor growth is dependent on metabolic state and metabolic support of stromal fibroblasts, highlighting these cells as attractive therapeutic targets in controlling cancer progression.

Appreciation

Every accomplishment in my life is a collection of effort and support from others. This dissertation is no exception. I want to especially express gratitude to Dr. Raghu Kalluri, who generously took me into his lab, never gave up on me and mentored me through the ups as well as downs of research. I benefitted from the warm friendships and advice of Dr. Valerie LeBleu, Dr. Joyce O'Connell, Dr. Vesselina Cooke, Dr. Sonia Melo, Dr. Sylvia Vong, Doruk Keskin, Cristina Espinosa, and other lab members. My work involved indispensable collaborators, namely Drs. Michael Zeisberg, Desiree Tampe, Manuel Esteller, Javier Carmona Sanz, Sughra Raza, John Asara, Marcia Haigis, and Karina Gonzalez. This dissertation would not be interesting without their contributions.

I sincerely thank Dr. David Frank, Dr. Lewis Cantley and Dr. Joan Brugge, my Dissertation Advisory Committee, for their guidance throughout the years. I also wish to thank my Dissertation Defense Committee, Dr. Bruce Zetter, Dr. Zoltan Arany, Dr. David Housman, and Dr. David Frank for graciously serving as my examiners.

Throughout my time at Harvard, I have received much support from Harvard Biological Biomedical Sciences Program and Division of Medical Sciences office, both faculty and administrators. Dr. David Cardozo and Dr. Connie Cepko have been caring and supportive during the unexpected interruption of my initial thesis research while Dr. Pat D'Amore has made me feel welcomed at Harvard during my first year of matriculation. I will not forget the fun discussions and many meaningful conversations with my fellow classmates in the program. Last but never least, I give many heartfelt thanks to my family and close friends. Their unconditional love and care are invaluable. Without them, I would never have come this far.

Thank you all from the bottom of my heart.

TABLE OF CONTENTS

LIST OF FIGURES AND TABLES

CHAPTER 1

BACKGROUND AND SIGNIFICANCE

Breast cancer incidence, development, diagnosis and treatment

Breast cancer has been one of the most prevalent cancers and one of the leading cancer killers of women worldwide (World Health Organization, 2009), especially in North America region (Figure 1). 1 in 8 U.S. women develops invasive breast cancer and there are ~230,000 new diagnosis with ~40,000 expected death in 2013 (Centers for Disease Control and Prevention, 2011; Susan G. Komen for the Cure, 2012). Although rare, ~2,200 expected diagnosis and ~400 deaths are expected for men in 2013 (Susan G. Komen for the Cure, 2012; Breastcancer.org, 2012). Since the development of mammography, more cases of breast cancer have been diagnosed at earlier stages where they can be successfully treated. During the 1980s and 1990s, incidence rate of early-stage breast cancer increased greatly and has remained stable while diagnosis of metastatic stage has dropped slightly (Susan G. Komen for the Cure, 2012). Between 1999 and 2005, total breast cancer incidence in U.S. women decreased by 2% per year due to the reduced usage of hormone replacement therapy (Breastcancer.org, 2012). However, breast cancer mortality rate has continued to increase for African American women (Susan G. Komen for the Cure, 2012).

Breast cancer develops in three major stages, from normal tissue to ductal carcinoma in situ to invasive ductal carcinoma and ends with metastatic disease (Polyak and Kalluri, 2010). The normal female breast structure includes the ductal epithelium and the myoepithelial cells surrounded by the basement membrane and separated from the connective tissue made up of fibroblasts, capillaries and extracellular matrix (Figure 2A). At early stage of cancer development, proliferation of transformed epithelial cells fills the lumen, forming ductal carcinoma *in situ* (DCIS). Other features of dysplastic lesion include increased number of blood vessels, dense extracellular matrix (ECM) and increased number of associating fibroblasts (Figure 2B). As breast cancer progresses, epithelial

cancer cells break free from the confinement of the basement membrane, forming areas with duct-like appearance, hence named invasive ductal carcinoma (IDC). Stromal environment contains many newly formed blood vessels, inflammatory factors and myofibroblasts (Figure 2C). In advanced stage, nearby tissue is affected with the invasion of cancer cells, evolving into metastatic disease (Figure 2D). Besides DCIS and IDC, other types of breast cancers include invasive lobular carcinoma, medullary carcinoma, mucinous (colloid) carcinoma, papillary carcinoma, tubular carcinoma, and inflammatory breast cancer (Susan G. Komen for the Cure, 2012).

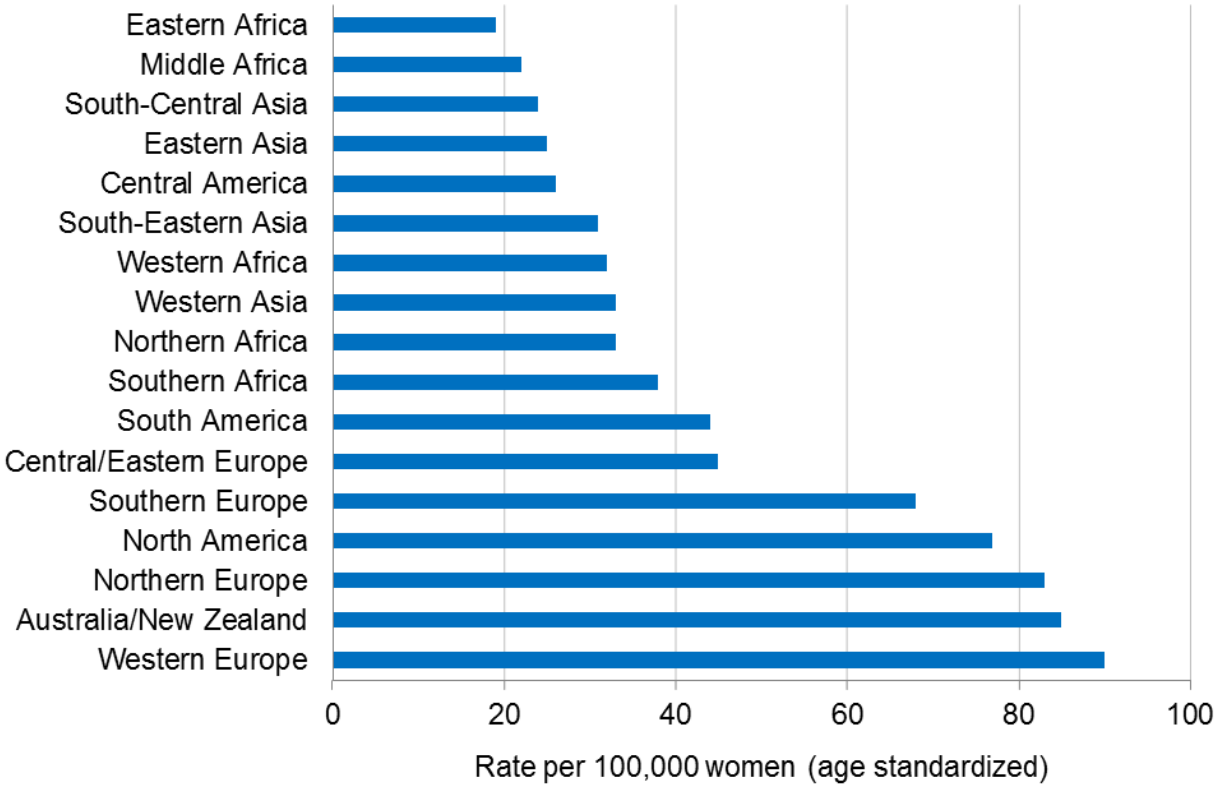

Figure 1. Women breast cancer incidence in the world with North America as one of the leading regions. Data from Forouzanfar et al. (2011).

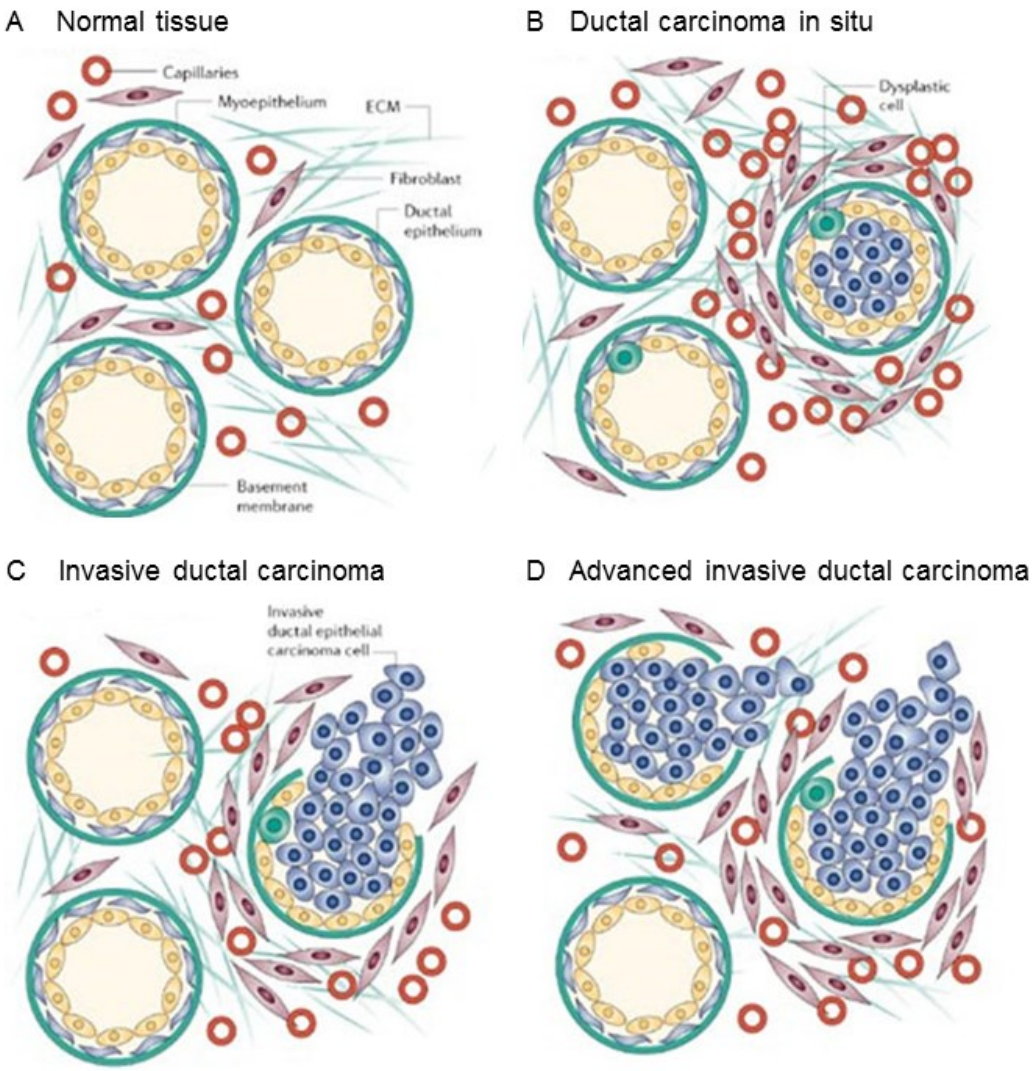

Figure 2. Stages of breast cancer development in human. (A) The normal female breast structure with organized ductal epithelium, myoepithelial cells, basement membrane, and connective tissue of fibroblasts, capillaries and extracellular matrix. (B) Proliferation of transformed epithelial cells in ductal carcinoma *in situ* (DCIS). (C) Invasive ductal carcinoma and (D) advanced invasive ductal carcinoma. Image is reproduced from Kalluri and Zeisberg (2006).

Breast cancer is usually first detected through physical examination or routine screening. Diagnosis can only be made through biopsy of the lump or abnormal area guided by appropriate imaging technologies – x-ray, ultrasound or MRI. Next, the biopsied tissue undergoes pathological evaluation. Staging of the diagnosis depends on the size and the location of the tumor, the number of affected lymph node, and whether metastasis has occurred. In general, there are 4 stages of breast cancers; DCIS at stage 0 and metastatic breast cancer at stage IV. Patients diagnosed with early stage breast cancer also undergo tests to predict metastasis probability, which is determined by lymph node and estrogen receptor status.

Women with familial history of breast cancer and/or have taken hormone replacement therapy are at higher risk for developing the disease. To choose appropriate treatment approach, molecular characteristics of the tumor are important. These include estrogen and progesterone receptor status, HER2/neu (ErbB2) status, and proliferation rate. Hormone receptor-positive breast cancers are often treated with hormone therapies, including Tamoxifen and aromatase inhibitors such as Anastrozole, Ietrozole or Exemestane (Susan G. Komen for the Cure, 2012). The principle is to prevent cancer cells from receiving the estrogen needed for tumor growth, either by lowering the estrogen level or by inhibiting the receptor. Hormone receptor-positive tumors have a lower chance of 5-year recurrence than negative tumors. HER2/neu-positive tumors represent about 15-20% of all breast cancers (Susan G. Komen for the Cure, 2012). For these tumors, treatment with the antibody Trastuzumab is effective (trade name: Herceptin). Monitoring of treatment often uses positron emission tomography (PET). PET scan utilizes radioactive glucose, which accumulates in extremely metabolic cells, a distinct characteristic of cancer cells.

Normal glucose metabolism versus the Warburg effect

In the past few years, cancer biology research has increasingly been attracted to metabolism and energy production in cancer cells. Under normal conditions, non-transformed cells rely on glucose for energy. Glycolysis pathway converts glucose into pyruvate, yielding 2 mol of ATP per mol of glucose (Figure 3A). Pyruvate is further shuttled through the tricarboxyclic acid cycle (TCA, also known as Krebs or citric acid cycle) inside the mitochondria (Lehninger et al., 2004) (Figure 3B). This process is coupled with oxidative phosphorylation and the electron transport chain to produce an additional 34 mol of ATP (Lehninger et al., 2004) (Figure 3B). Such high output of energy can only be possible in the presence of normal oxygen level. When oxygen is scarce or when cells are proliferating, glycolysis becomes the sole energy source. Lactate dehydrogenase converts pyruvate into lactate to regenerate NAD+ necessary for glycolysis to continue (Figure 4). Although this mode of energy production is far less productive than the TCA cycle and oxidative phosphorylation, it takes less time to generate ATPs. Moreover, intermediate metabolites from glycolysis can be used to produce nucleotides through the pentose phosphate pathway and to synthesize amino acids (Lehninger et al., 2004).

Interestingly, cancer cells prefer glycolysis coupled with lactate production even in abundance of oxygen (Figure 4). This phenomenon, named aerobic glycolysis or the Warburg Effect, was discovered by Dr. Otto Warburg while he observed cancer cells growing in vitro (Warburg et al., 1930). Unlike normal differentiated cells, cancer cells exhibit high glucose intake and high glycolysis rate. Substantial research over the past 80 years has revealed that one of the reasons cancer cells adopt aerobic glycolysis is due to oncogenes and tumor suppressors (Table 1). Many oncogenes including *PI3K*, *c-Myc* and *Ras* regulate glucose transport, glycolysis and TCA (Fritz and Fajas, 2010; Vander Heiden et al., 2009) while tumor suppressor p53 regulates the pentose phosphate pathway and

oxidative phosphorylation (Jones and Thompson, 2009). In addition, mutations in β-F1-ATPase and D-loop mitochondrial DNA, which likely impair oxidative phosphorylation, have been linked to poor prognosis in breast cancer (Isidoro et al., 2005; Tseng et al., 2006).

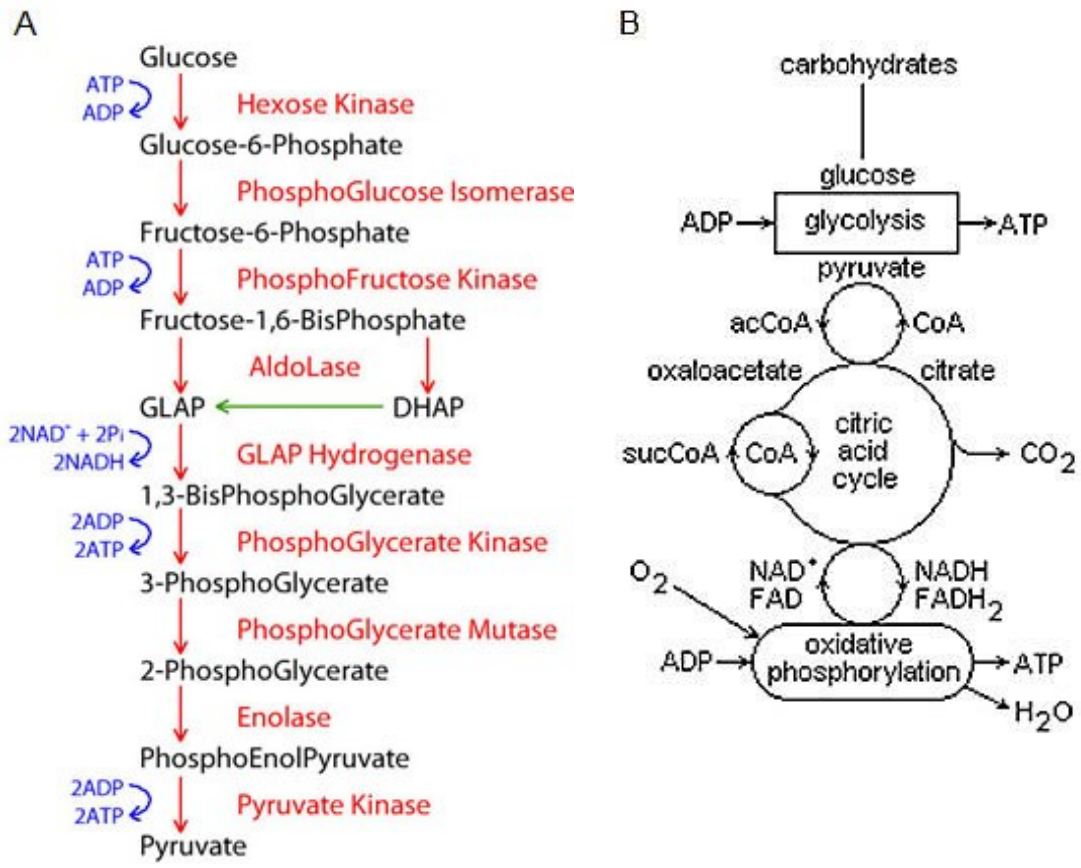

Figure 3. Diagrams showing glucose metabolism and energy production in normal, differentiated cells. (A) Glycolysis metabolizes glucose into pyruvate. (B) Pyruvate is shuttled through the TCA cycle, followed by oxidative phosphorylation and electron transport chain to produce ATPs. Images are reproduced from Biochem.co (2010).

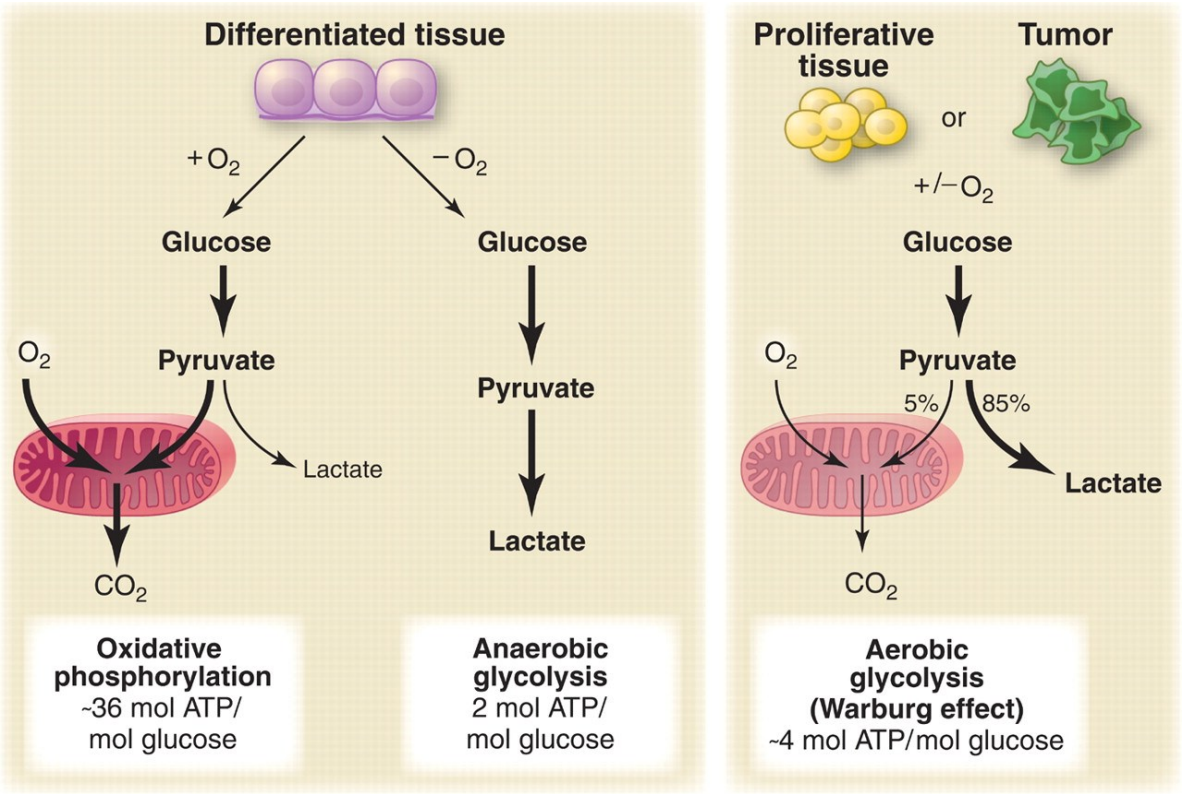

Figure 4. Glucose metabolism and energy production in normal versus tumor tissue. Differentiated tissues use glycolysis coupled with oxidative phosphorylation for high ATP output in normal oxygen. During hypoxia, lactate is produced following glycolysis to regenerate NAD+ necessary for continuing glycolysis. Proliferative tissue and cancer cells adapt to this alternative mode of metabolism even in normal oxygen. Image is reproduced from Vander Heiden et al. (2009).

Table 1. Table of oncogenes and tumor suppressors known to regulate metabolic pathways. Information from Fritz and Fajas (2010), Vander Heiden et al. (2009), Jones and Thompson (2009), and Shackelford and Shaw (2009).

Genes	Type	Metabolic pathways
p53	tumor suppressor	pentose phosphate, glucose uptake, oxidative phosphorylation
c-Myc	oncogene	glycolysis, glutaminolysis, TCA, nucleotide synthesis
PI3K/Akt	oncogene	glucose transport, glycolysis, fatty acid synthesis
Pten	tumor suppressor	glucose transport, glycolysis, fatty acid synthesis
Ras	oncogene	glycolysis
Lkb1	tumor suppressor	glycolysis

Some of the molecular metabolic consequences of oncogenes and tumor suppressors have been explored. Unlike differentiated cells, cancer cells increase glucose uptake by upregulating glucose transporter such as GLUT1 (Seyfried and Shelton, 2010; Vander Heiden et al., 2009; Koukourakis et al., 2006). Hexokinase (HK), which converts glucose into glucose-6-phosphate in the first step of glycolysis, is also highly upregulated (Seyfried and Shelton, 2010; Vander Heiden et al., 2009). Moreover, HK2 in particular is found to be expressed primarily in cancer cells (Seyfried and Shelton, 2010). The last step in glycolysis is pyruvate synthesis by pyruvate kinase (PK). Recently, Christoff et al. (2008) discovered that cancer cells switch from using pyruvate kinase isoform m1 (PKM1) to isoform m2 (PKM2) to efficiently shift their metabolism toward aerobic glycolysis (Christoff et al., 2008). Pyruvate, the resulting product, is metabolized into lactate by lactate dehydrogenase A (LDHA) and subsequently shuttled out of the cells through lactate exporter MCT4 (Seyfried and Shelton, 2010; Koukourakis et al., 2006). Extracellular lactate

can be taken back into the cells through lactate importer MCT1. However, MCT1 is usually downregulated, allowing the cancer cells to discard the accumulating intracellular lactic acid (Seyfried and Shelton, 2010; Koukourakis et al., 2006). Lactate dehydrogenase B (LDHB) which catalyzes the synthesis of pyruvate from lactate (Lehninger et al., 2004), is active in the normal liver but its expression and function in cancer cells remain unknown. Another important player is pyruvate dehydrogenase kinase (PDK). PDK resides inside the mitochondria and functions to prevent the entry of pyruvate into the TCA cycle by inhibiting pyruvate dehydrogenase (PDH) (Lehninger et al., 2004). In cancer cells, PDK1 and PDK4 are most often upregulated (Seyfried and Shelton, 2010). By upregulating key glycolysis enzymes and TCA cycle negative regulator, cancer cells are able to adopt aerobic glycolysis as their main mode of metabolism and energy production. A summary of the key enzymes involved in the Warburg effect is presented in Figure 5.

Pathways involved in glucose metabolism have been explored as potential targets for cancer therapy. Metabolic inhibitors such as dichloroacetic acid (DCA), 3-bromopyruvate acid (3BP) and 2-deoxy-d-glucose have been investigated clinically and seem to be promising anti-cancer agents (Seyfried and Shelton, 2010; Fulda et al., 2010). 3BP inhibits HK2 and DCA inhibits PDK while 2-deoxy-d-glucose prevents the uptake of functional glucose. Other potential targeting compounds include HK2 peptide and LDHA shRNA (Fulda et al., 2010).

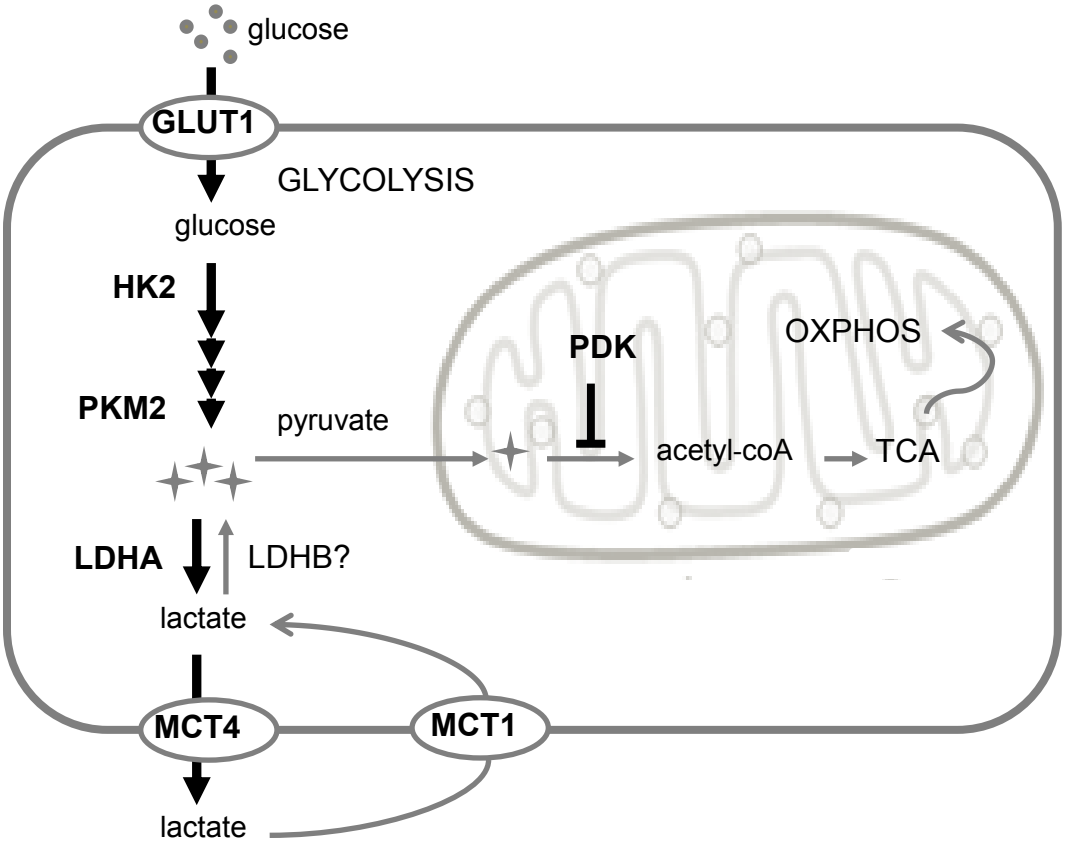

Figure 5. Altered glucose metabolism in cancer cells. Affected metabolic enzymes and transporters including GLUT1, HK2, PKM2, LDHA, PDK, MCT4 and MCT1 are shown in bolded letters. Information from Seyfried and Shelton (2010), Vander Heiden et al. (2009), Koukourakis et al. (2006), and Christoff et al. (2008).

Stromal fibroblasts in cancer

Fibroblasts are known to be special cells with spindle-like, mesenchymal appearance. Their role as regulators of ECM synthesis, structure and replacement in the connective tissues makes them the responsible cell type in the wound healing process. Fibroblasts are also found in excess in diseased settings such as organ fibrosis and cancers. Furthermore, fibroblasts of the same or different origins exhibit substantial

heterogeneity. To identify them, researchers rely on many protein markers such as vimentin, α-smooth-muscle-actin (αSMA), desmin, fibroblast-activation protein, and fibroblast-specific-protein 1 (Skalli et al., 1989; Schmitt-Graff et al., 1994; Sugimoto et al., 2006; Kalluri and Zeisberg, 2006). Expression of different combinations of these markers in fibroblasts has been observed in various pathological conditions. This characteristic pattern is believed to reflect the adaptation of fibroblasts to their environment.

A prominent subclass of fibroblast is the myofibroblast. These cells not only behave like fibroblasts, but also have contractility like smooth muscle cells (Gabbiani, 1992). Like smooth muscle cells, they express αSMA, which has become their distinct identification marker. Although the exact origin of myofibroblasts is controversial, it is now generally accepted that myofibroblasts can come from various sources. These include resident fibroblasts, bone marrow-derived progenitors and epithelial or endothelial cells. Resident fibroblasts are thought to expand and transdifferentiate into myofibroblasts while bone marrow-derived progenitors are recruited to the site prior to transdifferentiation. Recent emerging evidences suggest that myofibroblasts can come from mesenchymal transition of epithelial or endothelial cells (Hinz et al., 2007; Zeisberg et al., 2007). While normally rare, myofibroblasts are abundant in tumors, especially in high-grade malignancies and are associated with poor prognosis (Surowiak et al., 2007; Yamashita et al., 2012; Yazhou et al., 2004). Myofibroblast activation is thought to be unrestrained in the growing tumor, unlike the carefully regulated wound healing process in which they normally function. Due to this lasting response by the myofibroblasts, cancer is considered by many as a wound that never heals.

In breast cancer, stroma constitutes over 80% of the tumor mass (Dvorak, 1986). αSMA^+ myofibroblasts in tumors, also known as cancer-associated fibroblasts (CAFs), are the most prominent among the stromal cells. Research over many years have implicated

CAFs in tumorigenesis, tumor growth and progression. Although still controversial, there are some evidences suggesting the role of CAFs in tumor initiation. CAFs can stimulate tumor formation when co-injected subcutaneously with non-tumorigenic breast cancer cells lines in immunodeficient mice (Olumi et al., 1999). Additionally, neoplastic transformation is observed in epithelial cells from normal breast following overexpression of transforming growth factor β (TGFβ) or hepatocyte growth factor (HGF) in myofibroblasts (Kuperwasser et al., 2004).

CAFs are known to aid tumor growth and metastasis by providing growth factors and ECM remodeling proteins. They supply HGF and epithelial growth factor (EGF) which stimulate cell proliferation and promote resistance against apoptosis (Kalluri & Zeisberg, 2006). Many laboratories have shown that CAFs, not normal fibroblasts, substantially enhance tumor growth when co-injected with cancer cells (Orimo et al., 2001; Olumi et al., 1999; Kuperwasser et al., 2004). CAFs-derived matrix metalloproteinases (MMP), such as MMP-1, MMP-3, MMP-7 and MMP-11, degrade ECM and basement membrane, a crucial step in transitioning from carcinoma *in situ* to invasive carcinoma (Bisson et al., 2003; Hu and Polyak, 2008; MacDougall and Matrisian, 1995).

CAFs also play important roles in building blood vessels in the tumor. Pro-angiogenic factors such as vascular endothelial growth factor (VEGF), fibroblast growth factor 2 (FGF-2) and platelet-derived growth factors (PDGFs) are secreted by CAFs, mediating angiogenesis (Crawford et al., 2009; Dong et al., 2004; Hlatky et al., 1994; Fang et al., 2001). Increased tumor angiogenesis is observed in cancer xenografts co-injected with CAFs (Tuxhorn et al., 2002; Orimo et al., 2001). More importantly, myofibroblast-derived VEGF can compensate for the loss of VEGF in cancer cells (Dong et al., 2004).

CAFs express many pro-inflammatory cytokines and chemokines, recruiting immune cells to the tumor site as a result (Silzle et al., 2003; Allinen et al., 2004). By interacting and

facilitating communication among different cells in the tumors, these multitaskers mediate a permissive environment favorable for cancer cells in growth and progression. Figure 6 summarizes the numerous roles of CAFs in the tumor.

Given how active and different CAFs are compared to normal fibroblasts, it is expected that CAFs sustain genetic mutations. Patocs et al. (2007) noted *TP53* mutations in fibroblasts associated with sporadic breast carcinoma. However, following studies by Qiu et al. (2008), Campbell et al. (2008) and Hosein et al. (2010) all dispute this claim. Instead, there are evidences suggesting epigenetic changes. By analyzing global DNA methylation profiles using methylation-specific digital karyotyping, Hu et al. (2005) has identified altered DNA methylation patterns not only in tumor epithelial cells but also stromal fibroblasts. Another study testing for the presence of methylation in breast carcinoma CAFs has described particular DNA methylation of selected genes (Fiegl et al., 2006). In addition, stromal myofibroblasts isolated from human gastric cancers display global DNA hypomethylation (Jiang et al., 2008).

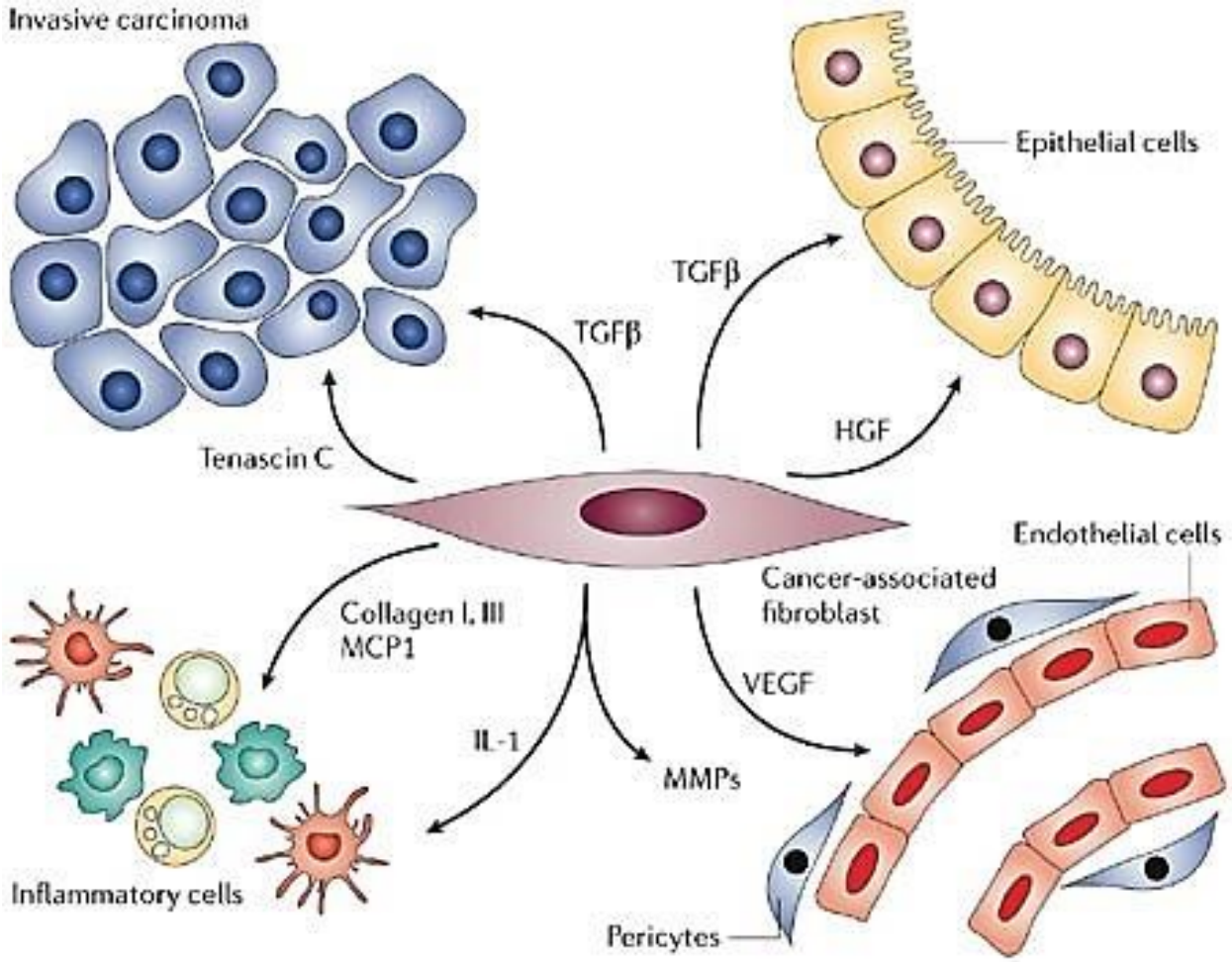

Figure 6. The multifunction of cancer-associated fibroblasts in the tumor. Image is reproduced from Kalluri and Zeisberg (2006).

Glucose metabolism in cancer-associated fibroblasts

Despite their major presence and contributing role in tumor progression, the metabolic state of CAFs remains unclear. The tumor environment contains an abundance of growth factors such as TGFβ, PDGF and FGF2 which can induce fibroblast proliferation (Polyak et al., 2010; Skobe et al., 1998; Bissell et al., 2001). Many have reported that CAFs are more proliferative than their normal counterparts *in vitro* and exist in much larger numbers in breast tumors versus adjacent normal tissues (Hawsawi et al., 2008; Rozenchan et al., 2009; Mercier et al., 2008; Shimoda et al., 2009). As described earlier in this chapter, proliferating cells display a different metabolic pattern than non-proliferating cells. In addition, the tumor microenvironment lacks oxygen and nutrients (Harris, 2002; Brown and Wilson, 2004; Pouysségur et al., 2006; Kallinowski et al., 1989; Vaupel et al., 1987). Hypoxia-induced factor 1α is known to transcriptionally induce expressions of GLUT1, HK2, PKM2, PDK1, LDHA and phosphofructokinase (PFK) in many cell lines including mouse embryonic fibroblasts (Semenza et al., 1994; Semenza et al., 1996; Ebert et al., 1995; Firth et al., 1995; Iyer et al., 1998; Yeung et al., 2008; Kim et al., 2006; Papandresu et al., 2006). The metabolic state of CAFs may be affected by such tumor microenvironment.

Our understanding of glucose metabolism in CAFs is limited. Koukourakis et al. (2006) examine colorectal adenocarcinoma tissues and show high expressions of MCT1 and LDHA, and low expression of GLUT1 in CAFs. For breast carcinoma, some interesting clues come from the research group of Michael Lisanti. In Caveolin-1 deficient murine bone marrow cells (which express myofibroblast-associated proteins), glycolysis enzymes such as GLUTs, PKM2, PGKL, LDHA, ALDOA, ENO1, TI1 and PGM1 are reportedly upregulated (Pavlides et al., 2009). hTERT-immortalized fibroblasts transformed with oncogenic H-Ras (G12V) display enhanced glycolysis and decreased protein expressions of oxidative

phosphorylation complexes II and V (Migneco et al., 2010). Knock down of mitochondrial transcription factor A (TFAM) in these cells shows loss of respiratory chain components, increased hydrogen peroxide and lactate, and promotes tumor growth in a xenograft model with MDA-MB-231 breast cancer cells (Balliet et al., 2011). In addition, MCT4 is expressed in normal fibroblasts upon exposure to MCF7 breast cancer cells (Whitaker-Menezes et al., 2011). Lisanti's group proposes a reverse Warburg effect model. In this model, CAFs (defined as Caveolin-1 knockout cells) are the cells that experience aerobic glycolysis in the tumor and CAFs-derived lactate and pyruvate are used by cancer cells to perform oxidative phosphorylation (Pavlides et al., 2009). Albeit interesting, the experimental approaches employed by the group contain serious caveats. Whether Caveolin-1 negative is a good marker for myofibroblasts is questionable. Caveolin-1, located at the cell membrane, plays a role in endocytosis and signal transduction (Razani et al., 2001; Couet et al. 1997; Lajoie and Nabi, 2010). Its knockout may change fundamental functions in cells such as metabolism. Oncogenic Ras and hTERT control important biological functions of cell proliferation and senescence respectively. Fibroblasts transformed with these genes are likely to behave differently.

Similar to other functions described earlier, glucose metabolism in CAFs may support tumor growth. A clear understanding of their metabolic role inside the tumors may provide new gateways to applicable therapies. In this dissertation, I first determine the metabolic differences between CAFs and normal fibroblasts, then explore the potential mechanisms which mediate such metabolic changes, and lastly examine the metabolic role of these cells in tumor growth.

CHAPTER 2

METABOLIC PROFILE OF CANCER-ASSOCIATED FIBROBLASTS

Work collaboration and contribution

The presented work involved indispensable collaborations. Human normal mammary fibroblasts and cancer-associated fibroblasts were grown from breast biopsies obtained as part of an institutionally approved clinical study in collaboration with *Dr. Sughra Raza* (Brigham and Women's Hospital, Boston). Metabolomics was done through collaboration with *Dr. John Asara* (BIDMC, Boston). Mitochondrial function tests were carried out in collaboration with *Dr. Marcia Haigis* (Harvard Medical School, Boston).

In addition, a number of individuals contributed to the work. In particular, I formulated the hypotheses and determined the experimental approach and direction together with my dissertation advisor *Dr. Raghu Kalluri*. *αSMA-RFP* mouse strain was generated by *Dr. Yingqi Teng* and *Dr. Joyce O'Connell* (BIDMC and Harvard Medical School, Boston). *Dr. Sylvia Vong* and *Dr. Joyce O'Connell* assisted with human fibroblast culture (BIDMC and Harvard Medical School, Boston). *Dr. Joyce O'Connell* also provided technical help with cancer cell implantation, RNA preparation for microarray and mtDNA content measurement. In addition, microarray data analysis, heat map generation and metabolomics data analysis were performed with her help. *Karina Gonzales* (Harvard Medical School, Boston) provided technical help by operating the XF24 Analyzer during mitochondrial function tests. I performed all remaining experiments.

Introduction

The tumor environment contains an abundance of growth factors such as TGFβ, PDGF and FGF2 which can induce fibroblast proliferation. Many have reported that fibroblasts are more proliferative and exist in much larger number in tumors than adjacent normal tissues (Skobe and Fusenig, 1998; Bissell and Radisky, 2001; Polyak and Kalluri, 2010). The tumor environment also lacks oxygen and nutrients due to the speedy growth of cancer cells (Harris, 2002; Brown and Wilson, 2004; Pouysségur et al., 2006; Kallinowski et al., 1989; Vaupel et al., 1987). The metabolic state of CAFs may be affected by such tumor microenvironment.

Our understanding of glucose metabolism in CAFs is limited. Koukourakis et al. (2006) examine colorectal adenocarcinoma tissues and show high expressions of MCT1 and LDHA, and low expression of GLUT1 in CAFs. For breast carcinoma, some interesting clues come from the research group of Michael Lisanti. In Caveolin-1 deficient murine bone marrow cells (which express myofibroblast-associated proteins), glycolysis enzymes such as GLUTs, PKM2, PGKL, LDHA, ALDOA, ENO1, TI1 and PGM1 are reportedly upregulated (Pavlides et al., 2009). hTERT-immortalized fibroblasts transformed with oncogenic H-Ras (G12V) display enhanced glycolysis and decreased protein expressions of oxidative phosphorylation complexes II and V (Migneco et al., 2010). Knock down of mitochondrial transcription factor A (TFAM) in these cells shows loss of respiratory chain components, increased hydrogen peroxide and lactate, and promotes tumor growth in a xenograft model with MDA-MB-231 breast cancer cells (Balliet et al., 2011). In addition, MCT4 is expressed in normal fibroblasts upon exposure to MCF7 breast cancer cells (Whitaker-Menezes et al., 2011). Lisanti's group proposes a reverse Warburg effect model. In this model, CAFs (defined as Caveolin-1 knockout cells) are the cells that experience aerobic glycolysis in the tumor and CAFs-derived lactate and pyruvate are used by cancer cells to perform oxidative

phosphorylation (Pavlides et al., 2009). Albeit interesting, the experimental approaches employed by the group contain serious caveats. Whether Caveolin-1 negative is a good marker for myofibroblasts is questionable. Caveolin-1, located at the cell membrane, plays a role in endocytosis and signal transduction (Razani et al., 2001; Couet et al. 1997; Lajoie and Nabi, 2010). Its knockout may change fundamental functions in cells such as metabolism. Oncogenic Ras and hTERT control important biological functions of cell proliferation and senescence respectively. Fibroblasts transformed with these genes are likely to behave differently. A direct comparison of unaltered endogenous CAFs and their normal counterparts is preferable.

In this chapter, we take a dual approach, utilizing unaltered human-derived fibroblasts and αSMA^+ fibroblasts isolated from mouse to understand the baseline metabolic differences between CAFs and normal fibroblasts. This information is the foundation for our mechanistic and functional studies.

Experiments and results

To determine whether CAFs exhibit altered metabolism, fibroblasts were directly isolated from normal mammary tissue and invasive ductal carcinoma of breast cancer patients and grown under aerobic conditions (37^oC, 5% CO_2, 20% O_2). We subjected these cells to a microarray analysis to identify potential differences in gene expression between CAFs (hCAFs) and normal (hNMFs). Pathway analyses of the data pointed to a differential gene expression profile in glycolysis, mitochondrial functions and oxidative phosphorylation (Figure 7A). Further assessment of the expression patterns demonstrated a trend for increased expression of genes involved in glycolysis. Transcriptional expression of key glycolysis genes *Glut1*, *Hk2*, *Pfkl*, *Pkm2*, *Ldha*, and lactate exporter *Mct4* by quantitative RT-PCR found that almost all of them were upregulated in hCAFs compared to NMFs

(Figure 7B). The amount of secreted lactate was significantly greater in hCAFs (Figure 7C), which was consistent with the increase *Mct4* expression (Figure 7B).

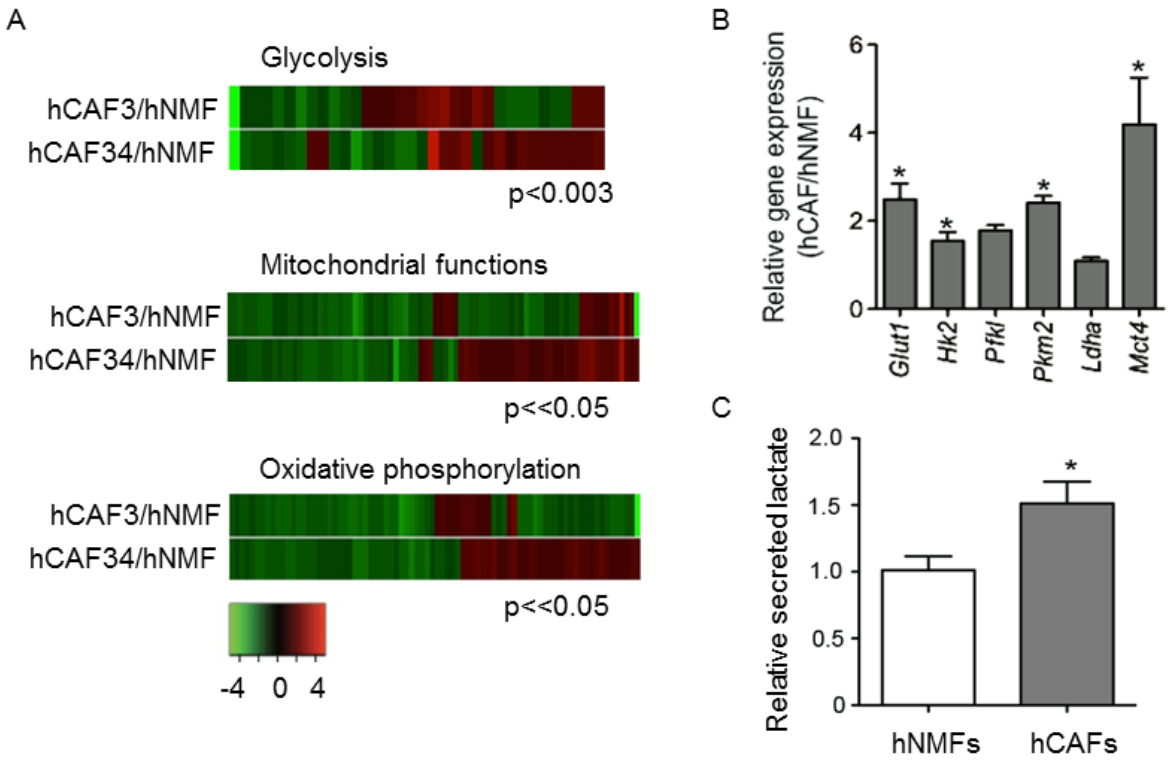

Figure 7. Comparison of metabolic gene expressions between CAFs and NMFs from human. (A) Microarray analysis of gene expressions in glycolysis, mitochondrial functions and oxidative phosphorylation pathways as defined by Ingenuity Pathway Analysis software. Heat maps represent gene expression of hCAF in comparison to hNMF, green indicates less and red indicates more detected mRNA. (B) Detection of important glycolysis enzymes and lactate exporter MCT4 by quantitative RT-PCR. (C) Relative concentration of lactate in the culture medium. Data are represented as mean ± SEM; *p<0.05.

Although hCAFs had increased glycolysis gene expressions, they might not have real functional effects. Thus, we performed targeted mass spectrometry to assess metabolite accumulations in both fibroblast groups. Metabolomic analyses revealed contrasting metabolite accumulations between hCAFs and hNMFs. In particular, hCAFs produced greater amounts of metabolites in glycolysis, mitochondrial functions, and oxidative phosphorylation (Figure 8A, 8B, and 8C, respectively). Interestingly, assays for oxygen consumption rate (OCR) and proton production rate (PPR) showed an increase trend in hCAFs compared to hNMFs (Figure 8E) without any difference in mitochondrial DNA content (Figure 8D). However, activities of the electron transport chain complexes hCAFs were ambiguous. Complex I seemed to be increased; complex IV seemed to be unchanging; and complex III seemed to be decreased (Figure 8F).

Figure 8. Comparisons of metabolites and mitochondrial functions between CAFs and NMFs from human. hNMFs and hCAFs were subjected to metabolomics studies. Relative abundance of each metabolite between hCAFs and hNMFs was calculated for glycolysis (A), mitochondrial functions (B) and oxidative phosphorylation (C) pathways as defined by Ingenuity Pathway Analysis software. (D) Relative mitochondrial DNA content between hCAFs and hNMFs. (E) Mitochondrial oxidative respiration activities in hCAFs compared to hNMFs: oxygen consumption rate (OCR, unit in pmoles/min/OD, $p=0.25$) and proton production rate (PPR, unit in pmoles/min/OD, $p=0.11$). (F) Electron transport chain complexes I, II and IV ($p=0.44$, $p=0.56$ and $p=0.65$ respectively). Data are represented as mean $\pm$ SEM; *$p<0.05$.

Figure 8 (continued)

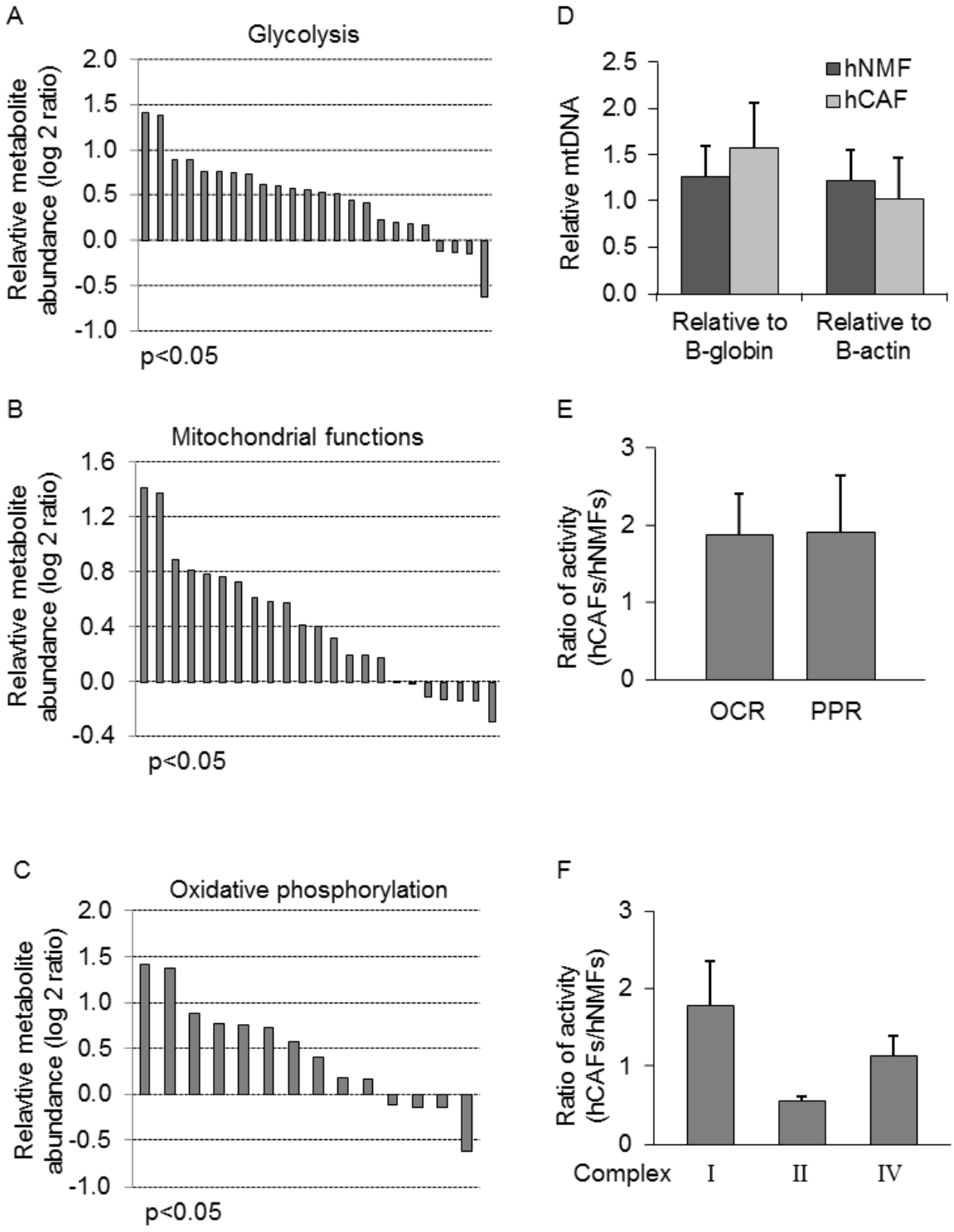

Another differential mitochondrial function between hCAFs and hNMFs is antioxidant activity. Cellular activities such as oxidative phosphorylation create various reactive oxygen species (ROS) as byproducts. Known ROS are superoxide anion, peroxide, hydrogen peroxide, hydroxyl radical and hydroxyl ion. One of the most important endogenous antioxidants against ROS, glutathione (GSH), functions by donating its reducing equivalents, becoming oxidized into glutathione disulfide (GSSG) in the process. Glutathione reductase (GR) keeps the system balanced by reducing GSSG back to GSH, allowing antioxidant activity to continue (Figure 9A). Human CAFs displayed a significantly higher ratio of GSSG to GSH with significantly less expression of GR than NMFs (Figure 9C and 9B, respectively). This data indicates defective antioxidant activity in CAFs.

For comparative studies, murine stromal fibroblasts from normal mammary tissue and mammary tumors were isolated from a transgenic mouse model in which the *αSMA* promoter drives the expression of red fluorescent protein (RFP). Isolated mouse fibroblasts were grown in aerobic condition (37^{o}C, 5% CO_2, 20% O_2) and then subjected to microarray, quantification of glycolysis gene expression and targeted mass spectrometry. Similar to human fibroblasts, pathway analyses of microarray pointed to a differential gene expression profile in glycolysis (Figure 10A). *Glut1*, *Hk2*, *Pfkl*, *Pkm2*, and *Ldha* were also upregulated in mCAFs compared to mNMFs (Figure 10B). Furthermore, metabolomic analyses uncovered that mCAFs likewise produce greater amounts of metabolites in glycolysis, mitochondrial functions, and oxidative phosphorylation (Figure 10C, 10D, and 10E, respectively).

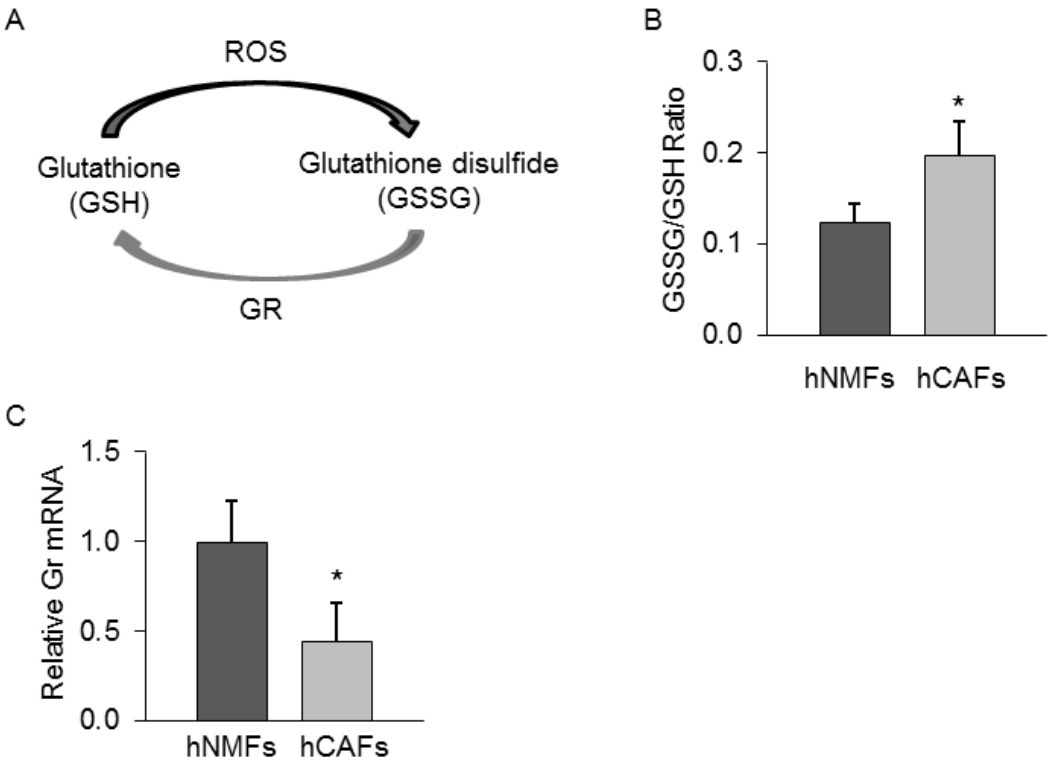

Figure 9. Decreased GR in hCAFs. (A) Schematic summarizing function of GR. Briefly, endogenous antioxidant GSH guarding against cellular ROS becomes oxidized into GSSG. GR converts GSSG back into GSH, allowing GSH to continue its antioxidant function. (B) GSSG and GSH in hNMFs and hCAFs were measured in metabolomic studies. Ratio of GSSG to GSH was computed for each group and graphed. (C) hCAFs contains significantly less *Gr* mRNA than hNMFs as detected by quantitative real time PCR. Data are represented as mean ± SEM; *p<0.05.

Figure 10. Comparison of metabolic profile between CAFs and NMFs from mouse. (A) Microarray analyses of gene expressions in glycolysis, mitochondrial functions and oxidative phosphorylation pathways as defined by Ingenuity Pathway Analysis software. Heat maps represent gene expression of mCAFs in comparison to mNMFs, green indicates less and red indicates more detected mRNA. (B) Detection of important glycolysis enzymes and lactate transporter by quantitative RT-PCR. mNMFs and mCAFs were also subjected to metabolomic studies. Relative abundance of each metabolite between hCAFs and hNMFs was calculated for glycolysis (C), mitochondrial functions (D) and oxidative phosphorylation pathways (E) as defined by Ingenuity Pathway Analysis software. Data are represented as mean $\pm$ SEM; *$p<0.05$.

Figure 10 (continued)

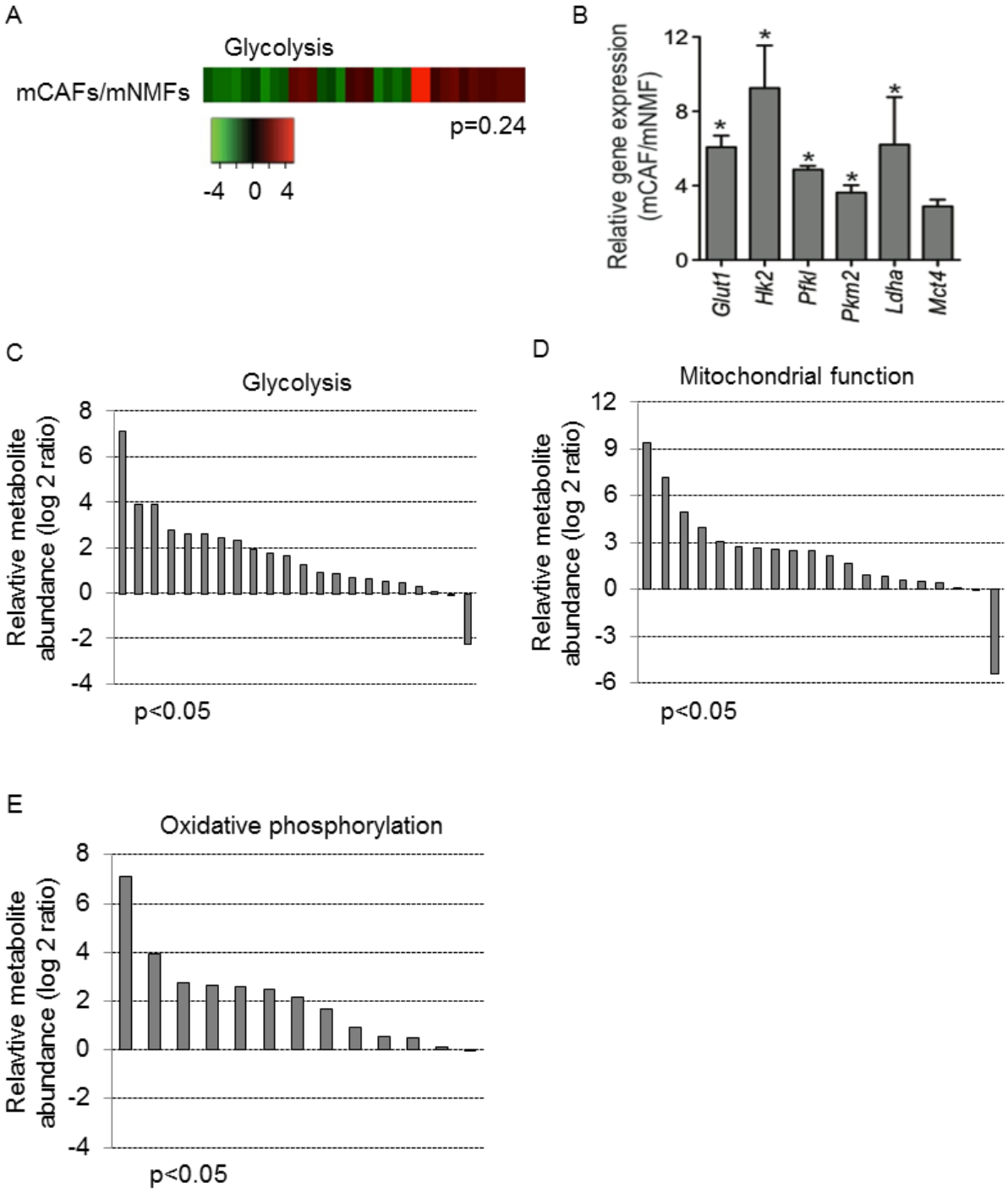

Discussion

Our different experimental approaches comparing breast CAFs to their normal counterparts from human and mouse support the hypothesis that stromal fibroblasts of the tumor microenvironment exhibit the Warburg effect. Their metabolic phenotype is defined as enhanced glycolysis activities and lactate production under aerobic conditions. In addition, CAFs seem to have increased oxygen consumption with defective antioxidant activity.

Our finding of ambiguous oxidative phosphorylation in CAFs surprisingly contradicts findings previously reported by the research group of Michael Lisanti. The observation made by the group that CAFs exhibit decreased mitochondrial oxidative phosphorylation may be specific to the Caveolin-1 knockout cell population. In addition, immortalized fibroblast cell lines that were transformed with oncogenic activated *Ras* were used in the experiments. Oncogenic *Ras* has been shown to not only alter glucose metabolism but also affect mitochondrial functions in mouse fibroblasts (Chiaradonna et al., 2006). In general, RAS controls a major signal transduction pathway that promotes cell growth and proliferation, consequentially affecting metabolism of the cells. These are possible explanations for the difference in our findings.

However, our examination of oxidative phosphorylation is not extensive. Activities of other electron transport chain complexes need to be assessed in order to obtain a complete picture of the entire pathway. It is possible that increase in cellular ROS (due to defective antioxidant activity and increase in oxygen consumption) may negatively affect the function of the protein complexes in the electron transport chain. Thus, the slowed pathway accumulates intermediate metabolites as a consequence.

Acknowledgement

This research was supported by grants from the National Institutes of Health DK55001, CA125550, CA155370, CA151925 and the Champalimaud Metastasis Programme (Dr. Raghu Kalluri); 5P01CA120964-05 and 5P30CA006516-46 (Dr. John Asara). I was supported in part by the Harvard Clinical and Translational Science Center training grant. Dr. Joyce O'Connell was supported by the Department of Defense Breast Cancer Research Predoctoral Traineeship Award (W81XWH-09-1-0008). Dr. Valerie LeBleu was funded from the NIH Research Training Grant in Gastroenterology (2T32DK007760-11). I would also like to thank Dr. David Frank, Dr. Lewis Cantley and Dr. Joan Brugge for their advice and helpful discussions.

CHAPTER 3

MECHANISMS OF METABOLIC ALTERATIONS IN CANCER-ASSOCIATED FIBROBLASTS

Work collaboration and contribution

The presented work involved indispensable collaborations. Human normal mammary fibroblasts and cancer-associated fibroblasts were grown from breast biopsies obtained as part of an institutionally approved clinical study in collaboration with *Dr. Sughra Raza* (Brigham and Women's Hospital, Boston). Methylation array and bisulfite sequencing were results from collaboration with *Dr. Manuel Esteller* (IDIBELL, Spain). Methylated DNA immunoprecipitation results were from collaboration with *Dr. Michael Zeisberg* (University Hospital Goettingen, Germany).

In addition, a number of individuals contributed to the work. In particular, I formulated the hypotheses and determined the experimental approach and direction together with my dissertation advisor *Dr. Raghu Kalluri*. *Dr. Joyce O'Connell* provided critical experimental design inputs. *Dr. Sylvia Vong* and *Dr. Joyce O'Connell* assisted with human fibroblast culture (BIDMC and Harvard Medical School, Boston). *Dr. Sonia Melo* (BIDMC, Boston) generously helped troubleshoot DNA purification protocol. Methylation data analysis and heat map generation help came from *Javier Carmona Sanz* (IDIBELL, Spain). Immunoprecipitation followed by PCR quantitation of *Fbp1*, *Pkm2* and *Hif1α* methylated DNA was performed by *Dr. Desiree Tampe* in the laboratory of *Dr. Michael Zeisberg* (University Hospital Goettingen, Germany). Quantitative real time PCR and immunoblot of *Hif1α* in hCAFs compared to hNMFs and treatment with 5-aza-2'-deoxycytidine were performed by *Dr. Valerie LeBleu* and *Dr. Joyce O'Connell* (BIDMC and Harvard Medical School). I performed all remaining experiments.

Introduction

Stromal cells isolated from normal and tumor tissue are known to maintain their differences even after prolonged cell culture and in xenograft studies (Bissell and Radisky, 2001; Tlsty and Hein, 2001; Orimo et al., 2005). The dramatic changes in gene expression patterns but lack of clonally selected somatic mutations in CAFs suggest potential epigenetic alterations (Qiu et al., 2008; Campbell et al., 2008; Hu and Polyak, 2008; Hosein et al., 2010). Indeed, by analyzing global DNA methylation profiles using methylation-specific digital karyotyping Hu et al. (2005) have identified altered DNA methylation patterns not only in the tumor epithelial cells but also in stromal fibroblasts. Another study testing for the presence of methylation in breast carcinoma CAFs has described particular DNA methylation of selected genes (Fiegl et al., 2006). In addition, stromal myofibroblasts isolated from human gastric cancers display global DNA hypomethylation (Jiang et al., 2008). Epigenetic changes in CAFs may explain the differential metabolic pattern reported in Chapter 2 of this dissertation.

Another potential mechanism for metabolic alterations in CAFs is hypoxia. The tumor environment lacks oxygen due to the fast growth speed of cancer cells. Hypoxia affects many cellular responses including the switch from oxidative phosphorylation to anaerobic glycolysis in normal cells. Most of glycolysis enzymes are transcriptional targets of HIF1α such as GLUT1, HK2, PFK, PKM2 and LDHA (Semenza et al., 1994; Semenza et al., 1996; Ebert et al., 1995; Firth et al., 1995; Iyer et al., 1998; Yeung et al., 2008). In multiple cell lines including cancer cells and mouse embryonic fibroblasts, PDK1 is a direct target of HIF1α, inhibiting pyruvate conversion into acetyl CoA at the beginning of TCA cycle (Kim et al., 2006; Papandresu et al., 2006). HIF1α has been established as a key player in the reprograming of metabolism in cancer cells and is being investigated as clinical therapy

(Semenza, 2010). With all its close connection to glucose metabolism, tumor hypoxia may be the trigger of Warburg effect in CAFs with HIF1α as a mediator.

Experiments and results

Epigenetic mechanism

To assess epigenetic changes in CAFs, we performed whole genome methylation array on the fibroblasts isolated and cultured from human breast biopsies. The high resolution array surveyed ~27,500 CpG islands utilizing close to 490,000 probes. Compared to hNMFs, hCAFs showed impressive contrasting differential patterns of methylation (Figure 11).

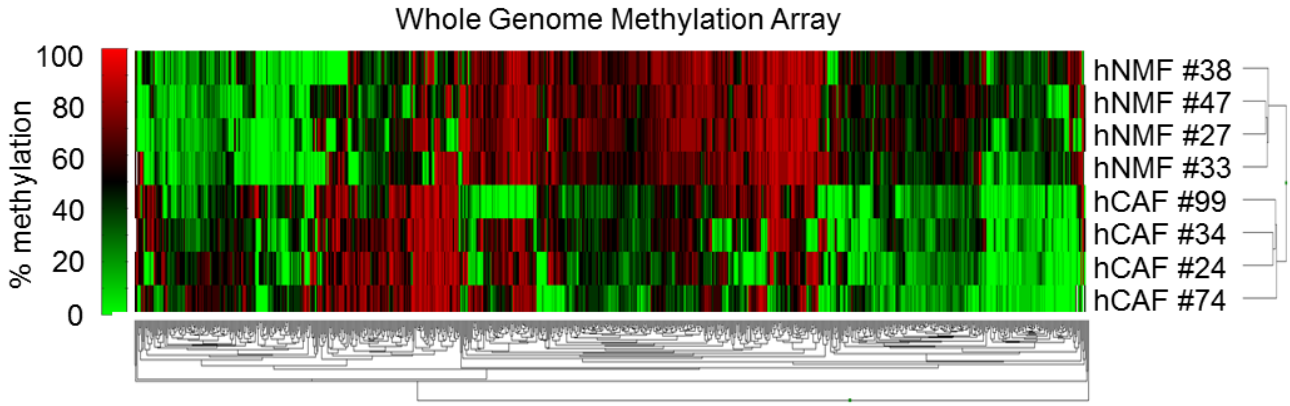

Figure 11. Whole genome methylation array comparing CAFs to NMFs. High resolution methylation array was performed to survey ~27,500 CpG islands on different hCAFs and hNMFs. Representative heat map shows impressive contrasting methylation patterns between CAFs and NMFs; unmethylated genes are shown in green and methylated genes are shown in red.

For glycolysis, 35 genes were significantly different at various DNA sites (Table 2). Gene methylation can occur at upstream of transcription start site, 5'UTR, 1st exon, gene body and even 3'URT regions at rare occasion. In epigenetic studies, only ~10% of methylation is usually correlated with gene expression for most regions. The 5'URT region, which often contains many gene expression elements, has up to 80% chance of correspondence to expression. Among the glycolysis genes which were differentially methylated in hCAFs compared to hNMFs, 6 genes had detected probes located in the 5'UTR region – *Fbp1*, *AldoB*, *Dhrs9*, *Aldh1B1*, *Pkm2* and *LdhB*. Between these genes, *Fbp1* and *Pkm2* attracted attention, being not only the rate limiting steps but also key regulatory enzymes of glycolysis. PKM2 (pyruvate kinase m2 isoform) regulates the synthesis of pyruvate from phosphoenolpyruvate, functioning as positive regulator of glycolysis. In contrast, FBP1 functions as a negative regulator of glycolysis, converting fructose-1,6 bisphosphate back to fructose-6-phosphate.

Table 2. Glycolysis genes differential methylated in CAFs. Data was extracted from whole genome methylation array. Table shows the gene region where differential methylation was detected including body, TSS200, TSS1500, 1st exon, 5'UTR and 3'UTR. Only genes with p-value of <0.05 are listed. Δ Methylation is the difference between hCAFs and hNMFs, shown as a percentage. For each gene, a positive numbers indicates a higher methylation and a negative number indicates lower methylation in hCAFs.

Table 2 (continued)

Genes	Region of Methylation	∆ Methylation	P-Value
ACSL1	Body	-19.00%	0.0349
ACSS1	TSS200	2.60%	0.0233
ACCSS2	Body;TSS1500	-15.00%	0.0168
ADH1B	TSS1500	-11.30%	0.0313
ADH6	TSS1500	-9.50%	0.0271
ADHFE1	Body	-8.60%	0.0297
ADHFE1	Body	3.30%	0.0054
ALDH1A3	Body	0.80%	0.0394
FBP1	**5'UTR**	**0.80%**	**0.0412**
ALDH1L1	Body	-7.90%	0.0451
ALDH3A2	Body	-5.50%	0.0457
ALDH3A2	Body	2.10%	0.0114
ALDH3B1	TSS1500	-6.20%	0.0422
ALDH3B1	Body	-10.20%	0.0074
ALDH3B1	TSS200	-9.50%	0.008
ALDH3B1	1stExon;5'UTR	-12.80%	0.0185
ALDH7A1	TSS200	1.70%	0.0414
ALDOA	TSS200;TSS1500;5'UTR	2.70%	0.0032
ALDOB	TSS1500	-12.40%	0.0079
ALDOB	5'UTR	-9.60%	0.0219
DHRS9	5'UTR;5'UTR	-6.00%	0.0384
DHRS9	TSS1500;5'UTR	-9.00%	0.0184
ENO3	TSS1500	3.80%	0.0436
ALDH1B1	5'UTR	-4.70%	0.0392
G6PC3	TSS1500	-9.50%	0.0257
G6PC3	TSS200	-0.40%	0.0346
GALM	TSS200	-4.80%	0.0434
GCK	Body	-14.40%	0.007
HK1	Body	9.40%	0.0379
HSD17B10	TSS200;TSS200	-9.00%	0.0289
LDHA	1stExon;5'UTR	-1.00%	0.0112
LDHAL6B	1stExon;Body	-3.80%	0.0446
PKM2	**5'UTR**	**-13%**	**0.0138**
PDHA1	1stExon; 5'UTR	-7.90%	0.0355
PFKFB1	TSS1500	-10.90%	0.0432

Table 2 (continued)

Genes	Region of Methylation	∆ Methylation	P-Value
PFKFB1	TSS1500	-7.60%	0.026
PFKFB3	Body	-8.60%	0.002
PFKFB3	Body	-1.90%	0.0431
PFKFB3	TSS200	-0.50%	0.047
PFKFB3	TSS200	-0.20%	0.0274
PFKFB3	TSS1500	7.40%	0.0026
PFKFB3	Body	2.10%	0.0172
PFKFB3	Body	5.30%	0.0089
PFKFB4	TSS1500	-0.70%	0.0443
PFKP	Body	3.00%	0.0468
PFKP	Body	3.70%	0.0422
PGAM2	TSS1500	14.90%	0.0145
PGK1	1stExon;5'UTR	-7.10%	0.0392
PGK2	TSS200	-6.50%	0.027
PGM5	3'UTR	-11.00%	0.0076
PGM5	Body	-6.60%	0.005
PKLR	TSS200;Body	-6.00%	0.0497
PKLR	TSS200;Body	-5.50%	0.0419
LDHB	5'UTR	-0.70%	0.0448
RDH14	TSS1500	1.30%	0.0461

In the case of *Pkm2*, hCAFs exhibited less methylation compared to hNMFs in the array with a difference of -13%, making it the 4th most differentially methylated gene detected in glycolysis. This hypomethylation was confirmed by methylated DNA immunoprecipitation (Figure 12A and B). In addition, *Pkm2* mRNA expression was significantly less in hNMF #33 which had the highest amount of methylated DNA; this suppression was attenuated by treatment with 5-aza-2'-deoxycytidine, an inhibitor of DNA methyltransferase (Figure 12C).

In the case of *Fbp1*, although the difference of methylation in the array was minimal, *Fbp1* was confirmed to be hypermethylated in hCAFs in two different validation methods, bisulfite sequencing of its promoter region (Figure 13A) and methylated DNA immunoprecipitation (Figure 13B and C). Furthermore, hypermethylation of *Fbp1* in hCAFs correlated with its decreased mRNA level which was rescued with the treatment of 5-aza-2'-deoxycytidine (Figure 13D).

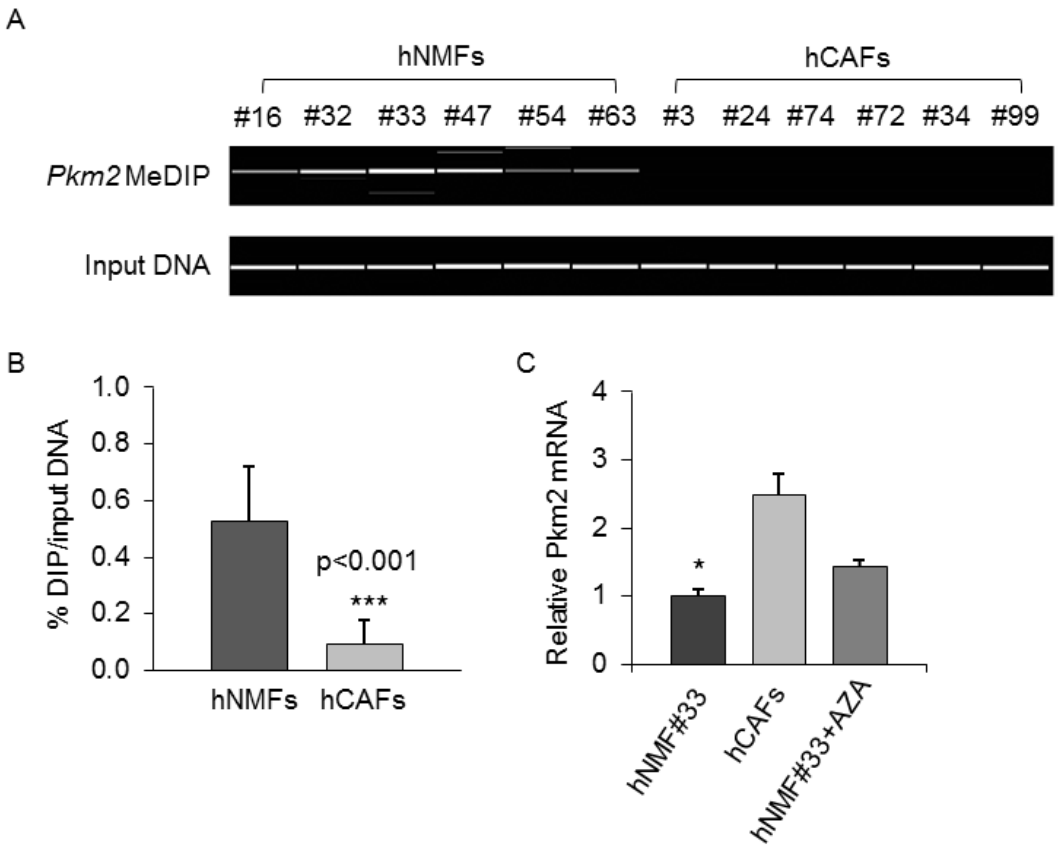

Figure 12. Hypomethylation of *Pkm2* in CAFs. Decreased methylation of *Pkm2* in hCAFs was detected by methylated DNA immunoprecipitation (MeDIP). Methylated DNAs were precipitated with 5-methyl-cytidine antibody from purified genomic DNAs and subjected to specific PCR. PCR gel image is shown in (A) and quantification of %DIP/input DNA is shown in (B). (C) shows the relative mRNA of *Pkm2* as measured by quantitative real time PCR in hNMF #33, hCAFs and hNMF #33 treated with 5-aza-2'-deoxycytidine (AZA). Data are represented as mean ± SEM; *p<0.05.

Figure 13. Hypermethylation of *Fbp1* in CAFs. (A) Bisulfite sequencing of 21 CpG islands in the promoter region. The methylation array included probes covering from the 6th island to the 9th island. Each square represents an individual sequenced clone. A filled square indicates methylation; an emptied square indicates unmethylation. Increased methylation of *Fbp1* in hCAFs was also confirmed with Methylated DNA Immunoprecipitation (MeDIP). Methylated DNAs were precipitated with 5-methyl-cytidine antibody from purified genomic DNAs and subjected to specific PCR. PCR gel image is shown in (B) and the quantification of %DIP/input DNA is shown in (C). (D) Relative mRNA of *Fbp1* as measured by quantitative real time PCR in hNMFs, hCAFs and hCAFs treated with 5-aza-2'-deoxycytidine (AZA). Data are represented as mean $\pm$ SEM; *$p<0.05$.

Figure 13 (continued)

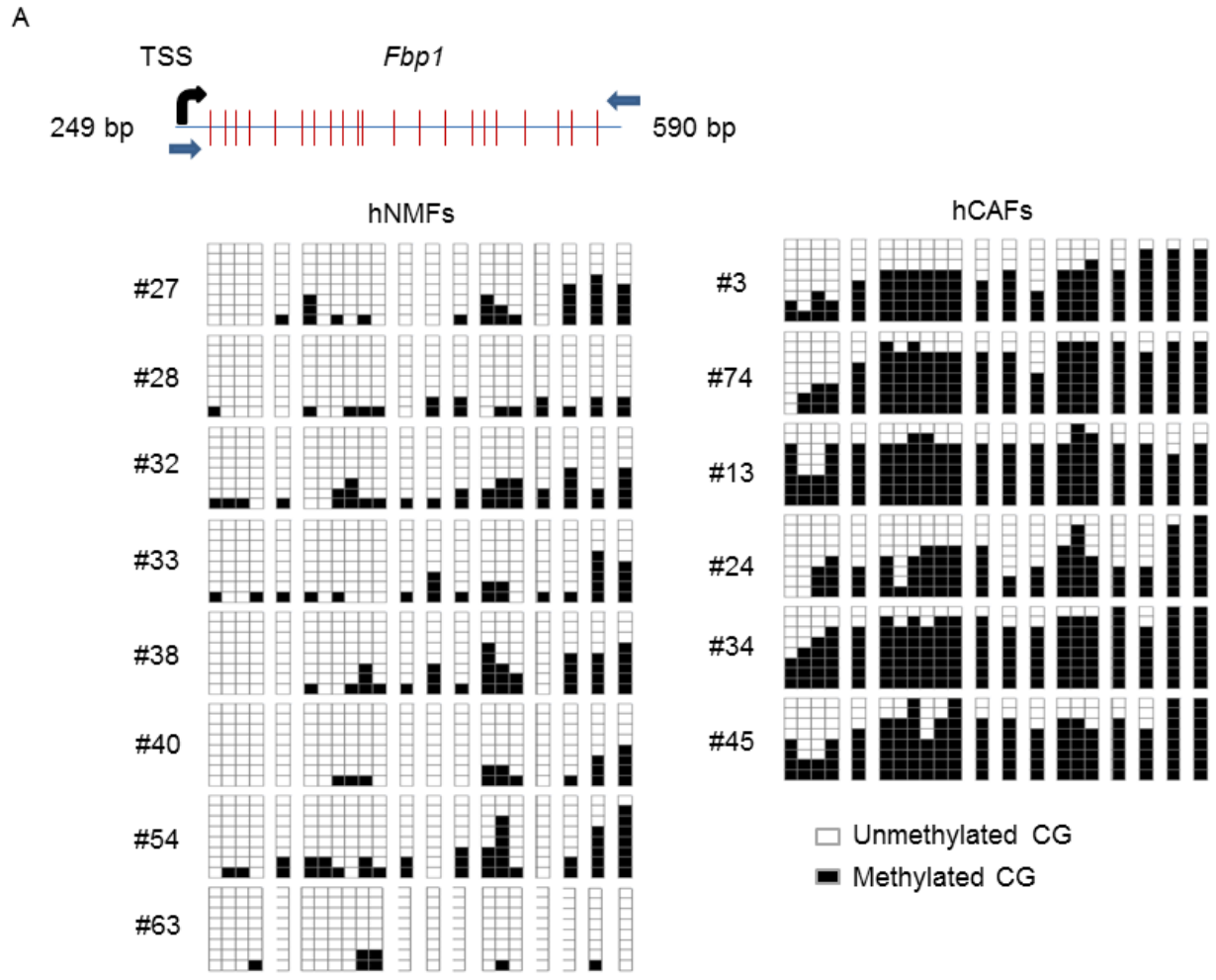

Figure 13 (continued)

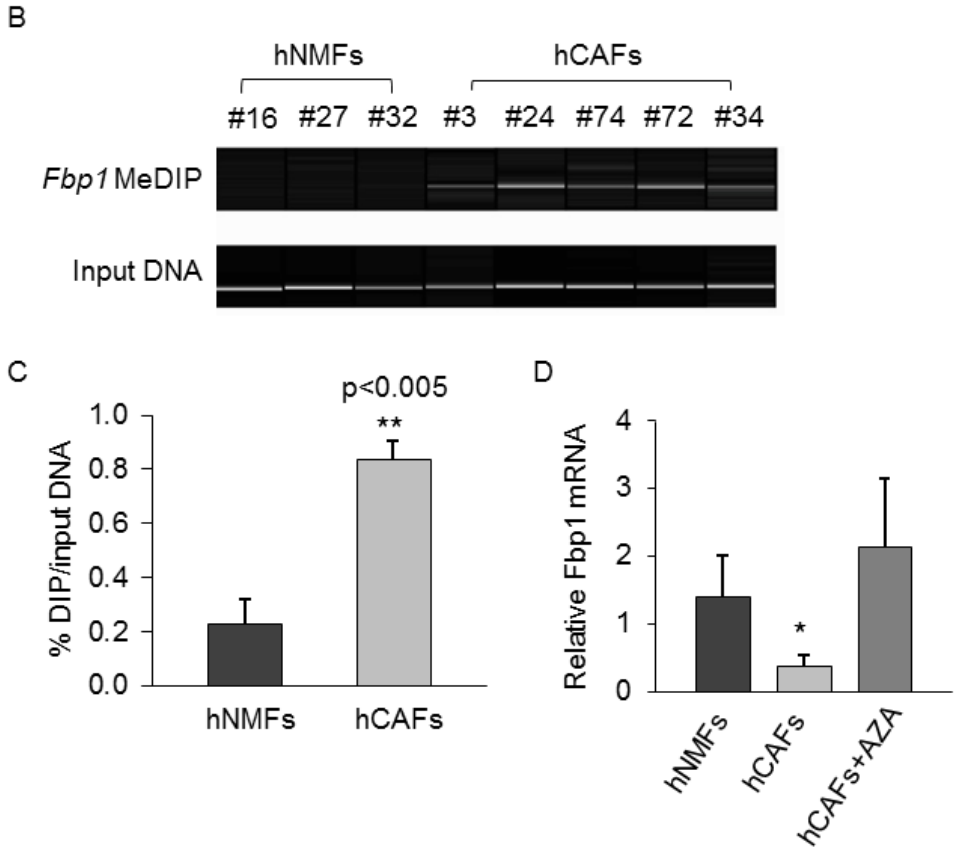

Hypoxia mechanism

First, to determine whether hypoxia can modulate expression of glycolysis enzymes in human breast fibroblasts, normal fibroblast cell line #21 was cultured in hypoxia (3% O_2) alternating with normal oxygen level (20% O_2) for 8 days and gene expressions were assessed with quantitative real time PCR. *Glut1*, *Hk2*, *Pfkl*, *Pkm2* and *LdhA* were affected with increased mRNA expressions coincided mostly with hypoxia (Figure 14A). As these glycolysis enzymes are transcriptional targets of HIF1α (Yeung et al. 2008) and our methylation array has indicated less methylation of *Hif1α* in hCAFs compared to hNMFs (mean difference 1.4%, p=0.015), methylation status of *Hif1α* in hNMFs exposed to hypoxia was assessed by methylated DNA immunoprecipitation. In 3 different hNMF cell lines #27, #32, and #54, *Hif1α* was sufficiently hypomethylated after 120 hours of chronic hypoxia (Figure 14B). Interestingly, this change was maintained despite reoxygenation for the next 24 hours (Figure 14B), suggesting that chronic hypoxia induced hypomethylation of *Hif1α* in fibroblasts.

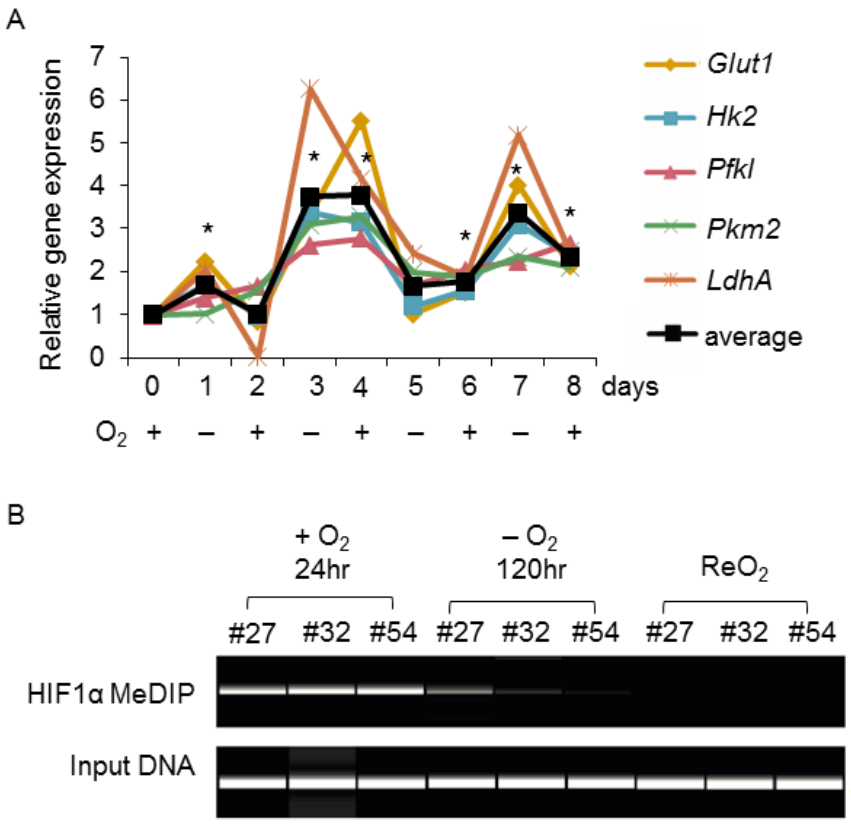

Figure 14. Hypoxia effect on expression of glycolysis genes and *Hif1α* methylation in NMFs. (A) hNMF #21 was subjected to hypoxia alternating with normal oxygen culture condition for 8 days and expressions of glycolysis genes *Glut1*, *Hk2*, *Pfkl*, *Pkm2* and *LdhA* were assessed by quantitative RT-PCR. The average of all 5 genes for each time point was also calculated and graphed. Hypoxia modulates expressions of all 5 genes. (B) 3 different hNMF cell lines, #27, #32 and #54 were subjected to hypoxia for 120 hours then reoxygenated for 24 hours and their *Hif1α* methylation status were assessed with methylated DNA immunoprecipitation. Methylated DNAs were precipitated with 5-methyl-cytidine antibody from purified genomic DNAs and subjected to PCR with *Hif1α* specific primers. Chronic hypoxia for 120 hours results in sustained decreased methylation of *Hif1α*. Data are represented as mean ± SEM; *p<0.05.

If hypoxia in fact induces permanent hypomethylation of *Hif1α*, *Hif1α* mRNA level should remain elevated in spite of longer reoxygenation. To test this hypothesis, hNMFs #32 and #54 were exposed to hypoxia for different durations of 24, 72, 120, and 168 hours each followed with reoxygenation for 48 hours. Cells were collected at different time points for assessment of mRNA and proteins to compare *Hif1α* expressions. Longer reoxygenation was designed deliberately to determine whether increased *Hif1α* mRNA and protein would still be maintained. As expected, hypoxia induced a significant increase of *Hif1α* mRNA and protein compared to baseline level (0hr) in both tested cell lines (Figure 15A and B). More importantly, the mRNA continued to increase in reoxygenation post hypoxia and this increase was only observed after 120 hours of hypoxia but not at earlier time points (Figure 15A). HIF1α protein accumulated in hypoxia and remained relatively unchanged after reoxygenation (Figure 15B and C). These results strongly suggest that prolonged hypoxia can induce stable and likely permanent expression of *Hif1α* mRNA and protein in fibroblasts.

In the context of a tumor, fibroblasts exposed to chronic hypoxia undergo *Hif1α* hypomethylation, leading to stable and prolonged gene expression and consequently inducing its transcriptional targets including glycolysis enzymes. According to this mechanism, *Hif1α* in hCAFs should be less methylated and its mRNA and protein should be higher in hCAFs than in hNMFs. In fact, none of the hCAFs tested showed methylation PCR band while all of the hNMFs did (Figure 16A). Quantification of the band intensities confirmed significant hypomethylation in hCAFs (Figure 16B). In addition, detected mRNA was ~1.7 fold higher in hCAFs (Figure 16C). Although Hif1α protein levels varied between different cell lines (Figure 16D), hCAFs showed more HIF1α when normalized by loading control (Figure 16E). These data suggest that *Hif1α* can be a contributing factor to the enhanced glycolysis in CAFs we observed in chapter 2 of this dissertation.

Figure 15. Chronic hypoxia induces stable expression of *Hif1α*. hNMFs #32 and #54 were subjected to hypoxia for different durations (24, 72, 120, and 168 hours) followed by reoxygenation for 48 hours. (A) *Hif1α* mRNA was assessed with quantitative RT-PCR. Graphs represent fold difference relative to baseline of 0hr. *Hif1α* at baseline is significantly less compared to all conditioned samples. (B) Western blots comparing hypoxia and reoxygenation samples detected 3 bands of molecular weights 100-120KDa. All band intensities were quantified with NIH ImageJ software and average HIF1α/ACTIN ratios were calculated for comparison (C). Significant increase in HIF1α protein in all samples is observed when compared to baseline but no difference between hypoxia and reoxygenation samples is detected. Data are represented as mean ± SEM; *$p<0.05$.

Figure 15 (continued)

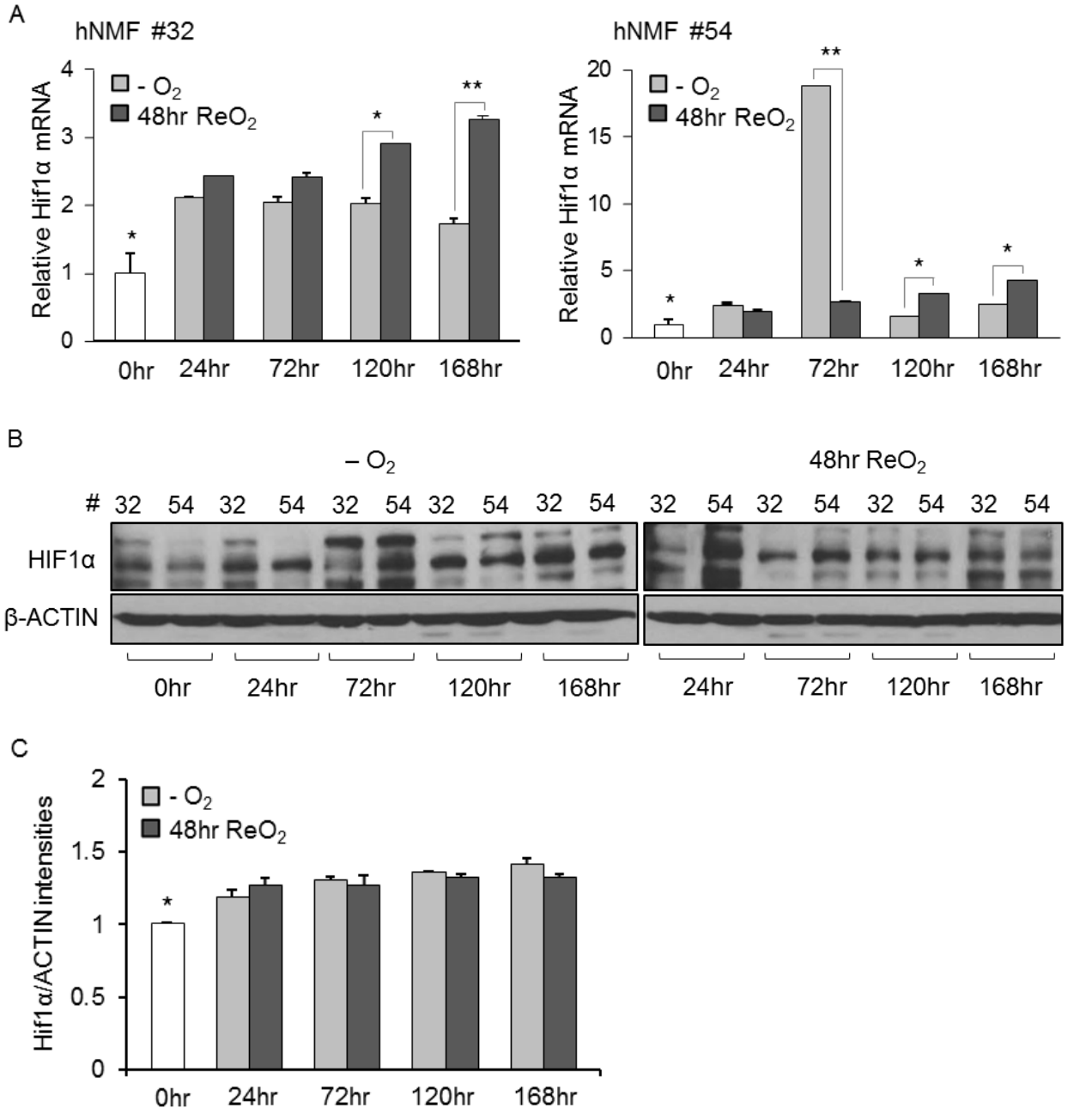

Figure 16. Methylation status and expression of *Hif1α* in CAFs versus NMFs. (A) Comparison of *Hif1α* methylation between hNMFs and hCAFs by methylated DNA immunoprecipitation. Methylated DNAs were precipitated with 5-methyl-cytidine antibody from purified genomic DNAs and subjected to PCR with Hif1α specific primers. PCR gel image (A) and quantification of %DIP/input DNA (B) show hypomethylated *Hif1α* in hCAFs. (C) *Hif1α* mRNA expression is more in hCAFs compared to hNMFs per quantitative RT-PCR assessment. (D) HIF1α protein levels were assessed with Western blot. Intensities of all 3 bands of 100-120KDa were quantified with NIH ImageJ software and average Hif1α/Tubulin ratios were calculated for comparison (E). hCAFs exhibit ~2 fold more HIF1α protein than hNMFs. Data are represented as mean ± SEM; *$p<0.05$.

Figure 16 (continued)

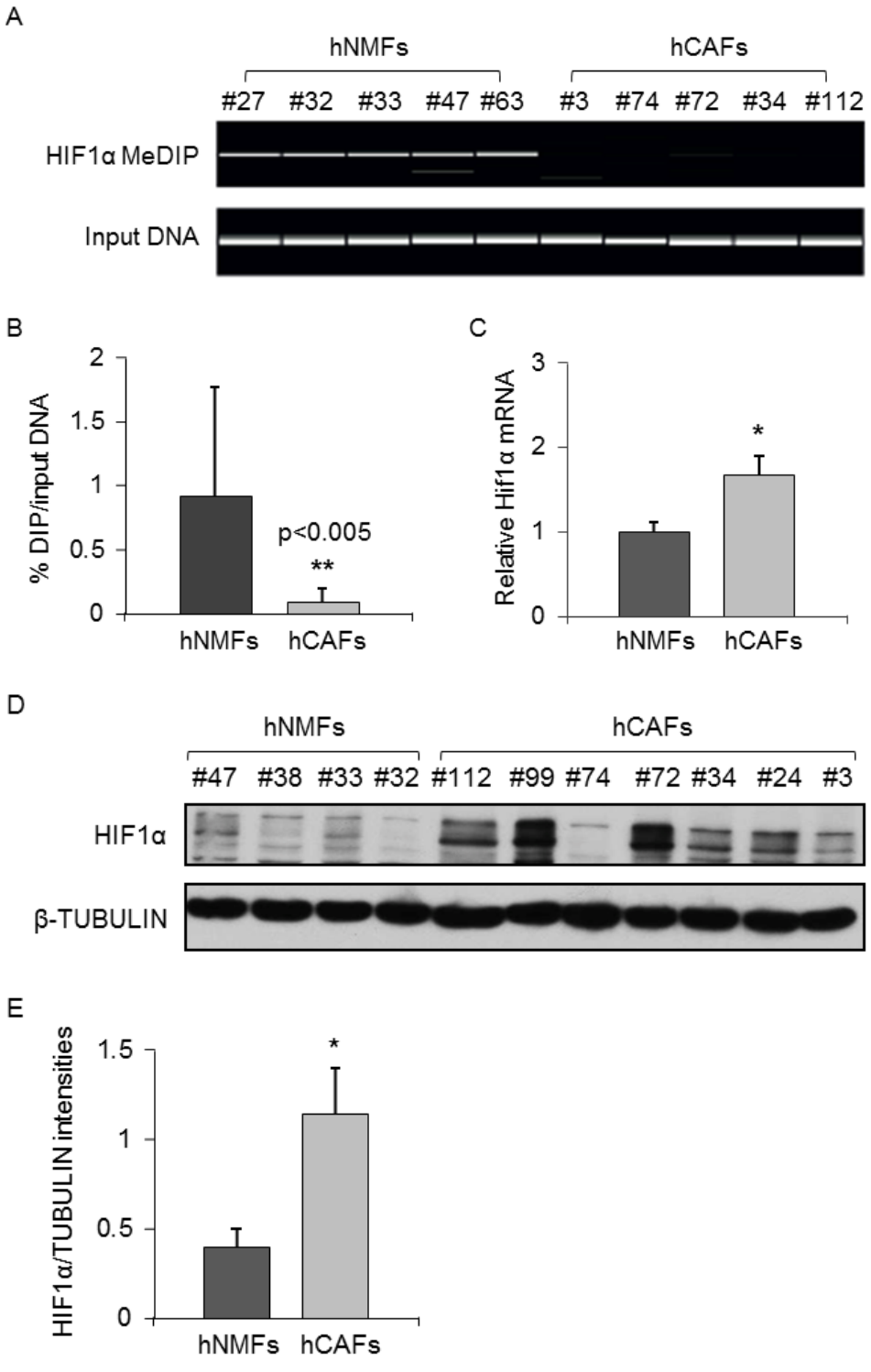

Discussion

In this chapter, our experiments explore and support two mechanisms of Warburg effect in CAFs. Firstly, enhanced glycolysis may be due to hypermethylation of negative regulators such as *Fbp1* and hypomethylation of positive regulator such as *Pkm2*. Secondly, chronic hypoxia can manipulate glycolysis gene expressions via inducing hypomethylation of *Hif1α*. Investigation reveals that hNMFs lost methylation of *Hif1α* when deprived of oxygen for as little as 4 to 5 days. Reoxygenation up to 48 hours does not reverse this loss. Moreover, sustained *Hif1α* methylation change upon chronic hypoxia correlates with its increased mRNA and protein expressions.

Our data demonstrate an upregulation of *Pkm2* in stromal fibroblasts of the tumor microenvironment. *Pkm2* expression in cancer cells has been previously implicated in the regulation of tumor metabolism (Christofk et al., 2008) and its inhibitors are being researched. If the 4T1 cancer cell line used in our study does not express *Pkm2*, the designed drugs will likely target tumor-promoting stromal fibroblasts in *Pkm2* negative cancers. Whether this will be effective therapy is worth exploring.

The studies presented here suggest that tumor hypoxia, a driver for expression of glycolysis and lactate production genes (Denko, 2008; Semenza, 2010), likely influences stromal fibroblasts along with cancer cells. Similar to muscle cells in the body, fibroblasts experiencing oxygen starvation exhibit increased production and removal of cellular lactate. Another possible explanation is that cancer cells directly induce metabolic changes in their tumor constituents. Whether cancer cells induce metabolic changes in fibroblasts independent of general tumor oxidative stress deserves a separate investigation.

Our studies also discover that stromal fibroblasts undergo epigenetic alterations that possibly contribute to their sustained Warburg phenotype in the context of a growing tumor. Besides *Fbp1* and *Pkm2*, other metabolic genes in CAFs may have undergone similar

epigenetic modifications. Most methylation studies of metabolic genes in cancer have focused on cancer cell lines of the corresponding carcinoma, suggesting that hypermethylation or hypomethylation of important metabolic genes take place in the cancer cells (Wolf et al., 2011; Goel et al., 2003; Xu et al., 2012). Our results provide the first evidence that similar epigenetic modifications also exist in cancer-associated fibroblasts. Tumor hypoxia is again a likely contributing factor, having been shown to induce loss of global methylation in normal human dermal fibroblasts (Shahrzad et al., 2007).

More importantly, we uncover a direct involvement of tumor hypoxia in regulating metabolic reprogramming in stromal fibroblasts - hypomethylation of *Hif1α*. Speculations in the field have favored epigenetic alterations as an explanation for the vast differences between CAFs and normal fibroblasts. Our experiments identify cancer cell-induced hypoxia as the potential initiator of a chain of epigenetic modifications, and ultimately, also responsible for changing the metabolic profile of neighboring stromal fibroblasts to favor tumor growth. These results demonstrate the need for more attention to hypoxic regions in tissues during cancer screening, and suggest the avoidance of hypoxia as a potential method for cancer prevention.

Acknowledgement

This research was supported by grants from the National Institutes of Health DK55001, CA125550, CA155370, CA151925 and the Champalimaud Metastasis Programme (Dr. Raghu Kalluri); 5P01CA120964-05 and 5P30CA006516-46 (Dr. John Asara). I was supported in part by the Harvard Clinical and Translational Science Center training grant. Dr. Joyce O'Connell was supported by the Department of Defense Breast Cancer Research Predoctoral Traineeship Award (W81XWH-09-1-0008). Dr. Valerie LeBleu was funded from the NIH Research Training Grant in Gastroenterology (2T32DK007760-11). I would also like to thank Dr. David Frank, Dr. Lewis Cantley and Dr. Joan Brugge for their advice and helpful discussions.

CHAPTER 4

FUNCTIONAL CONTRIBUTION OF METABOLIC ACTIVITIES IN STROMAL FIBROBLASTS TO TUMOR GROWTH

Work collaboration and contribution

The presented work involved indispensable collaboration. Metabolomics was done through collaboration with *Dr. John Asara* (BIDMC, Boston).

In addition, a number of individuals contributed to the work. In particular, I formulated the hypotheses and determined the experimental approach and direction together with my dissertation advisor *Dr. Raghu Kalluri*. *αSMA-tk* mouse strain was generated by *Dr. Yingqi Teng* and *Dr. Joyce O'Connell* (BIDMC and Harvard Medical School, Boston). Cancer cell implantation, tumor measurements and immunostaining for *αSMA-tk* treated with GCV were performed by *Dr. Joyce O'Connell* (BIDMC and Harvard Medical School, Boston). She also helped with metabolomics data analysis and heat map generation. Technical help with *Pdk* knockdown and PCR confirmation came from *Dr. Valerie LeBleu* (BIDMC and Harvard Medical School). I performed all remaining experiments.

Introduction

CAFs have been shown to provide growth factors such as TGFβ, cytokines such as IL-1 and ECM remodeling proteins such as MMPs to aid tumor growth and metastasis (Kalluri and Zeisberg, 2006). The metabolic status of CAFs may play a role in aiding tumor metabolism. Supporting evidence includes significant inhibition of tumor growth by 2-deoxy-D-glucose and DCA in xenograft model of MDA-MB-231mammary epithelial cancer cells co-injected with Cavelin-1 knockout fibroblasts (Bonuccelli et al., 2010). Indeed, Pavlides et al. (2009) have hypothesized that the Warburg effect in CAFs provides adjacent cancer cells with energy-rich metabolites such as lactate and pyruvate. In a xenograft mouse model using MDA-MB-231, synthetic glycolysis fibroblasts overproduce lactate and promote tumor growth independent of angiogenesis (Balliet et al., 2011). In addition, oncogenic Ras-transformed fibroblasts exhibiting Warburg phenotype enhance tumor growth of MDA-MB-231 (Migneco et al., 2010). Decreased tumor growth has been observed in a lung mouse model and xenograft human colorectal cancer following treatments with a small molecule inhibitor of MCT1 (Sonveaux et al., 2008). However, there is no direct evidence to address the role of glucose metabolism inside CAFs in tumor growth.

In this chapter, we first assess the functional contribution of αSMA^+ myofibroblasts to the overall metabolic status and growth of the tumor. Subsequently, we focus on the importance of lactate uptake in cancer cells and more importantly the intricate changes to the tumors when the Warburg effect in CAFs is attenuated. These experiments ensure a clear approach in determining the contribution of metabolic activities in stromal fibroblasts to tumor growth.

Experiments and results

To assess the functional contribution of αSMA$^+$ myofibroblasts to the overall metabolic status and growth of the tumor, we used a reported transgenic mouse model to enable the specific ablation of αSMA$^+$ myofibroblasts (Tse, 2011). In this transgenic mouse model, the *αSMA* promoter drives the expression of viral thymidine kinase (*tk*), such that ganciclovir (GCV) administration into *αSMA-tk* mice results in the signification depletion of αSMA$^+$ cells (Figure 17A and B, reported by Tse, 2011). The loss of myofibroblasts significantly reduced tumor growth (Figure 17C and D, reported by Tse, 2011). The depletion of αSMA$^+$ myofibroblasts also decreased the overall levels of glycolysis metabolites in the tumors including lactate, indicating that stromal fibroblasts are important contributors to the glycolysis activities of the tumor as a whole (Figure 18A and B). In addition, we separately assessed metabolites from the cancer cells isolated from αSMA-tk tumors. Surprisingly, cancer cells from αSMA-tk also showed a pattern of decreased metabolite accumulation similar to the overall tumors (Figure 18C and D). This experiment suggests that in association with diminished tumor growth the loss of stromal myofibroblasts can attenuate the Warburg effect within the cancer cells and the tumor as a whole.

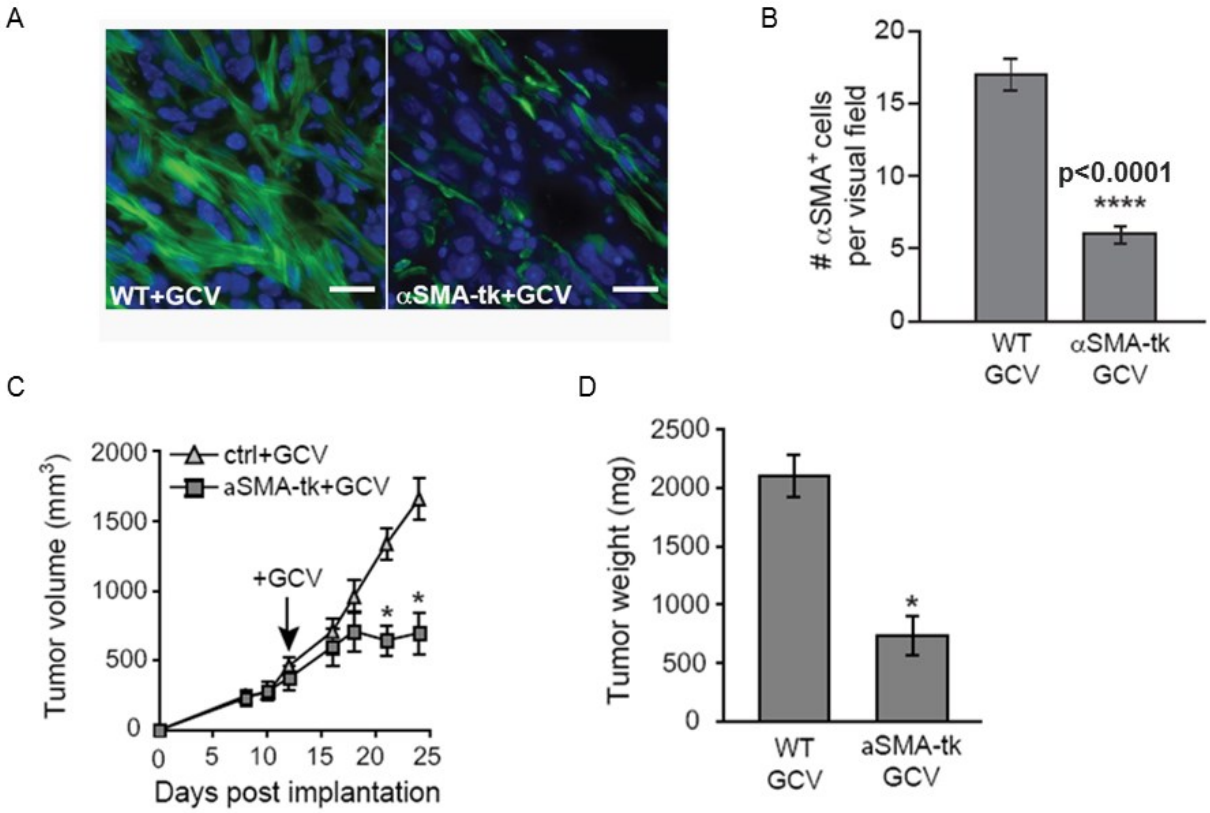

Figrue 17. Ablation of αSMA$^+$ myofibroblasts in *αSMA-tk* mice results in decreased tumor growth. 4T1 murine mammary epithelial cancer cells were implanted into the breast pads of either wildtype or *αSMA-tk* mice. (A) Staining of αSMA in tumors (αSMA in green, cell nuclei in blue), show the expected ablation effect following GCV treatment at day 12 post implantation. (B) Quantification of αSMA$^+$ cells per visual field confirms significant ablation in stained tumors. Attenuated tumor volume (C) and weight (D) are observed in ganciclovir-treated *αSMA-tk* mice (αSMA-tk+GCV) compared to control mice (WT+GCV). Data are represented as mean ± SEM; *p<0.05. (A) and (B) are reproduced from doctoral dissertation of Tse (2011) with permission.

Figure 18. Ablation of αSMA^{+} myofibroblasts in *αSMA-tk* mice affects metabolism in tumors and cancer cells. Metabolomics was performed on whole tissues (A) or 4T1 cancer cells isolated from αSMA-tk+GCV and WT+GCV mice (C) from Figure 17. Heat maps (A) and (C) indicate differential metabolite accumulations in fibroblast-ablated tumors. Data for glycolysis were extracted; relative abundance was calculated as ratios between αSMA-tk+GCV and WT+GCV for each metabolite (B and D). Analysis using Ingenuity Pathway Analysis software indicates significant different glycolysis not only between αSMA-tk+GCV and WT+GCV tumors but also between their respective isolated 4T1 cancer cells.

Figure 18 (continued)

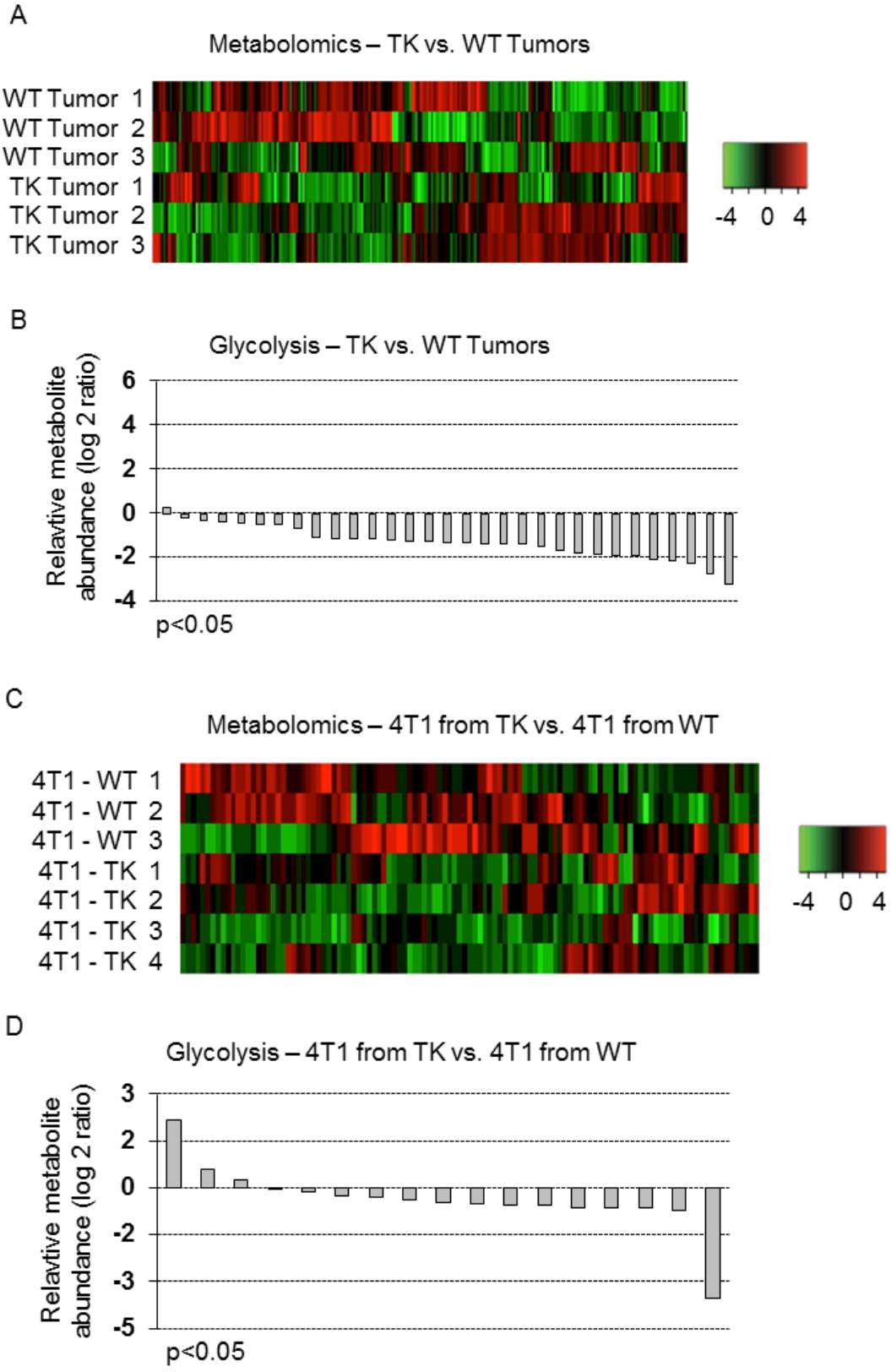

The results of the *αSMA-tk* experiment suggest that the Warburg effect in stromal fibroblasts supports the Warburg effect in cancer cells. Lactate may be one of the mediators, being decreased in cancer cells of *αSMA-tk* tumors. To test this hypothesis, we targeted lactate production in fibroblasts and lactate uptake in cancer cells. Firstly, we knocked down *Pdk* in mouse embryonic fibroblasts (MEF) using shRNA prior to co-injection with 4T1 cancer cells into breast pads of mice. PDK inhibits entry of pyruvate into the TCA cycle. Consequently, the suppression of *Pdk* shifts glucose metabolism away from lactate production. Quantitative RT-PCR confirmed the significant downregulation of all *Pdk* genes in MEF+shPdk cells (Figure 19A). Lactate production was also significantly attenuated in these cells (Figure 19B), while no discernible differences in cell proliferation between *Pdk* silenced and control fibroblasts were observed. Co-injection of 4T1 cancer cells with *Pdk*-knockdown fibroblasts resulted in decreased tumor growth (Figure 19C and D). Protein levels of GLUT1, HK2, PKM2, and LDHA were decreased in the knockdown tumors (Figure 19E). When tumors were examined as a whole, metabolomic analysis demonstrated a decrease in most glycolysis metabolites including lactate (Figure 19F). Assessment of the metabolic profile of the cancer cells isolated from these tumors determined that *Pdk* suppression in fibroblasts also lead to decreased glycolysis metabolites in the cancer cells (Figure 19G). Although the stromal fibroblasts were manipulated to decrease lactate production, the affected cancer cells also shifted their glucose metabolism to less lactate production.

Figure 19. Shifting glucose metabolism away from lactate specifically in stromal fibroblasts impedes tumor growth and suppresses the Warburg effect in cancer cells. (A) Quantitative RT-PCR for *Pdk* expression in mouse embryonic fibroblasts expressing *Pdk*-targeting shRNA (MEF+shPdk) relative to control MEF. (B) Quantification of lactate levels in the culture media. (C) MEF+shPdk or control MEF was co-injected with 4T1 cancer cells and tumor volume was measured over 21 days. (D) Tumor weights at experimental endpoint. (E) Representative immunoblot of tumor lysates with antibodies against GLUT1, HK2, LDHA and PKM2. Metabolomics was performed on total tumor tissues (F) and tumor-derived 4T1 cancer cells (G) from MEF+shPdk and control tumors. Data for glycolysis were extracted; relative abundance was calculated as ratios between MEF+shPdk and control MEF for each metabolite. Analysis using Ingenuity Pathway Analysis software indicates significant different glycolysis not only between MEF+shPdk and control tumors but also between their respective isolated 4T1 cancer cells. Data are represented as mean $\pm$ SEM; *$p<0.05$.

Figure 19 (continued)

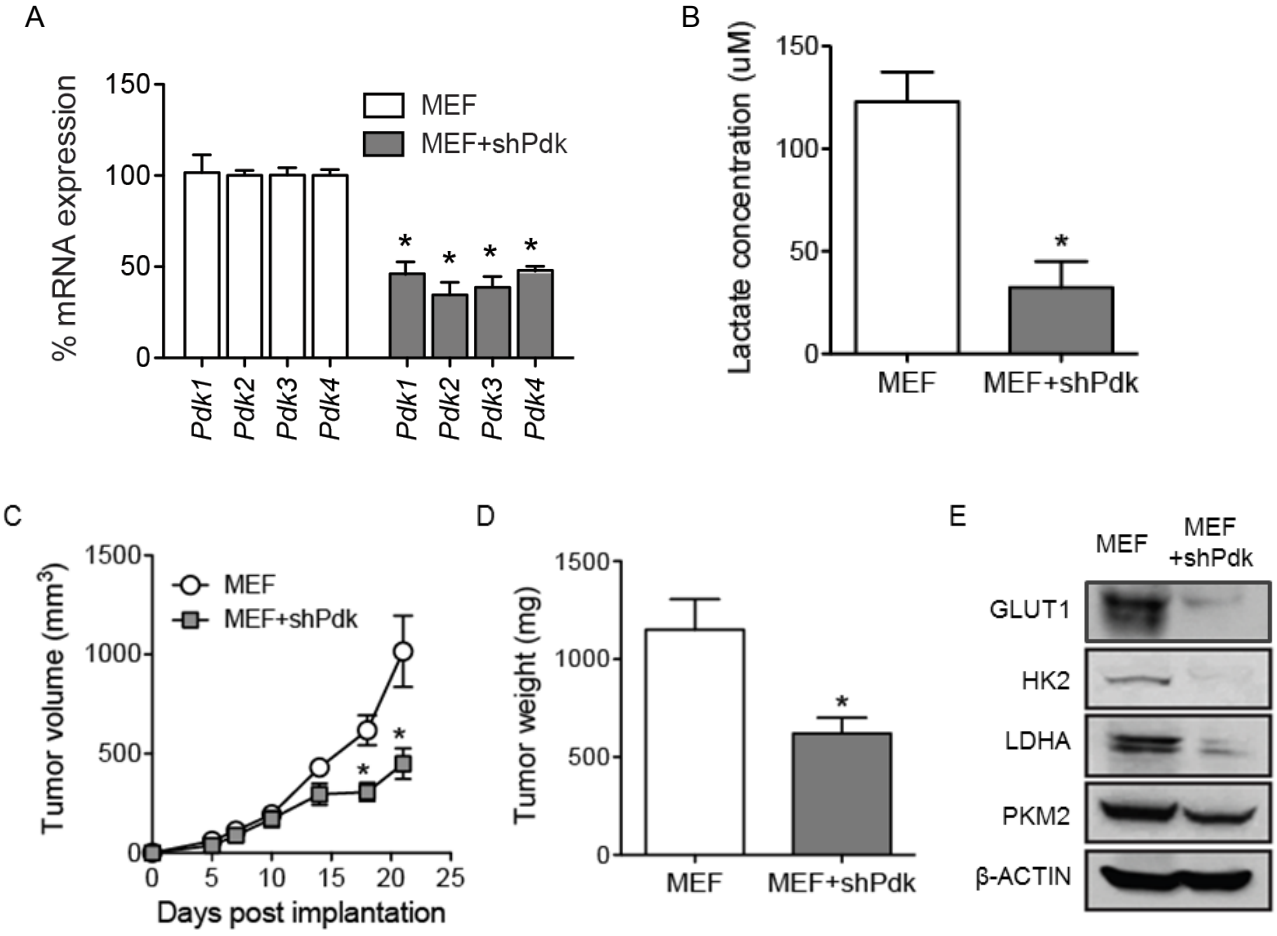

Figure 19 (continued)

F

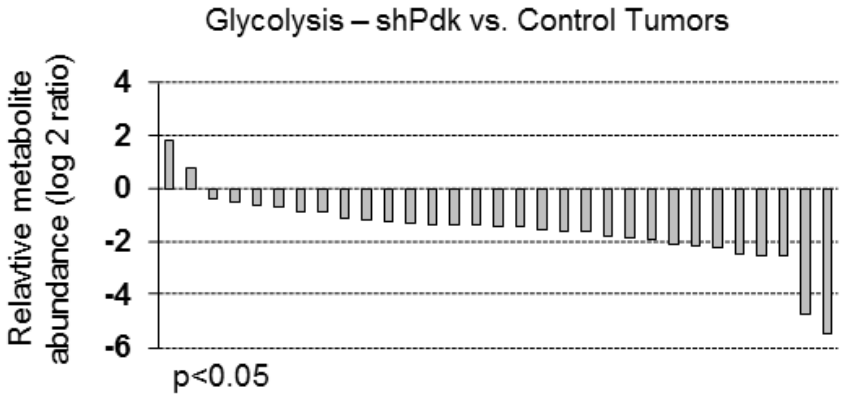

G

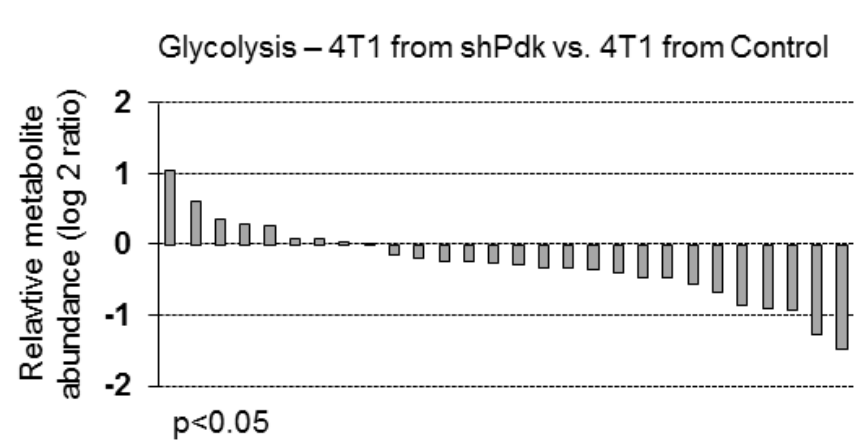

4T1 cancer cells were subjected to *Mct1* knockdown by shRNA prior to injection into breast pads of mice. Quantitative RT-PCR confirmed the downregulation of *Mct1* in 4T1 transfected with shMct1 (Figure 20A) and *Mct1* knockdown resulted in significantly decreased tumor growth (Figure 20B and C). This finding is consistent with previous reports of decreased tumor growth observed in a lung mouse model and xenograft human colorectal cancer following treatments with small molecule inhibitor of MCT1 (Sonveaux et al., 2008).

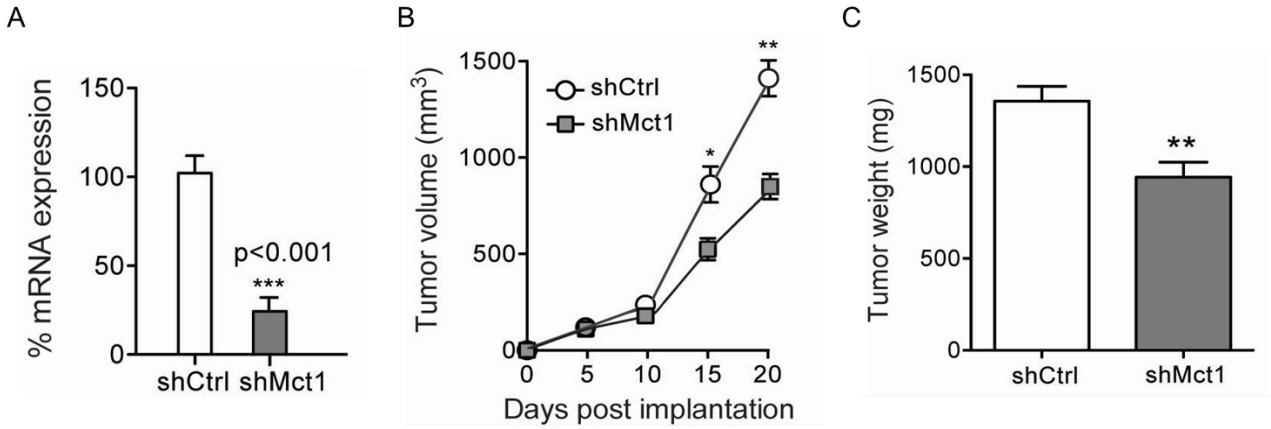

Figure 20. Inhibition of lactate uptake in cancer cells results in decreased tumor growth. 4T1 cancer cells were transfected with either control shRNA (shCtrl) or *Mct1* shRNA (shMct1) prior to orthotopic implantation in mice. (A) Quantitative RT-PCR for *Mct1* expression in transfected cells. (B) Comparative tumor volumes were measured over 20 days. (C) Tumor weights at experimental endpoint. Data are represented as mean ± SEM; *p<0.05.

Discussion

Our *αSMA-tk* experiment is the first evidence that CAFs contribute to the overall metabolism ongoing in the tumors. Furthermore, knockdown of *Pdk* in fibroblasts and *Mct1* in cancer cells supports the notion that the Warburg effect in CAFs assists tumor growth, likely through the provision of lactate.

Combined, these data suggest that stromal fibroblasts contribute to the growth of tumors via direct metabolic support of the cancer cells. While others have demonstrated that the co-injection of highly glycolysis fibroblasts with cancer cells can increase tumor growth (Migneco et al., 2010), our studies specifically reveal that fibroblasts with increased lactate production will also increase lactate in cancer cells. *Pdk* suppression experiment suggests that the metabolic status of stromal fibroblasts is essential to tumor growth. Dichloroacetate (DCA), which inhibits the activity of PDKs and increases pyruvate utilization by the TCA cycle, has been explored as a possible cancer therapeutic in a few mouse studies (Bonnet et al., 2007; Sun et al., 2010). Preliminary assessment indicates that DCA exhibits anti-tumor effects in clinical trials (Michelakis et al., 2010). Our data suggests that the anti-tumor effects of DCA can also be due to its impact on stromal fibroblasts in the tumor.

This study not only showcases the importance of metabolic functions of fibroblasts in tumor growth, but also calls for more emphasis in learning about glucose metabolism in tumor stromal constituents. Currently, there is no information on the metabolic states of pericytes, endothelial cells, epithelial and inflammatory cells in the context of tumors. These cells are active stromal components and known to contribute in different steps of tumor growth and progression. It is likely that they also contribute metabolically to the tumors, may be even compensate for the metabolic activities in cancer cells in the absence of fibroblasts.

These are important questions which regretfully cannot be covered under the scope of this dissertation.

Recently, Fiaschi et al. (2012) have explored the metabolic reprogramming in fibroblasts exposed to prostate cancer cells. Although the cancer type is different than ours, the findings are similar. Exposed fibroblasts display Warburg phenotype, increased glucose uptake, and lactate production and secretion (Fiaschi et al., 2012). Pharmacologic inhibition of MCT1 in cancer cells strongly inhibits cell survival as well as prostate tumor growth (Fiaschi et al., 2012). This raises the question of whether metabolic reprogramming in fibroblasts is the same disregarding cancer type. Such information will help determine whether anti-metabolism is a relevant therapeutic option and further personalize cancer treatment for individual patients.

Acknowledgement

This research was supported by grants from the National Institutes of Health DK55001, CA125550, CA155370, CA151925 and the Champalimaud Metastasis Programme (Dr. Raghu Kalluri); 5P01CA120964-05 and 5P30CA006516-46 (Dr. John Asara). I was supported in part by the Harvard Clinical and Translational Science Center training grant. Dr. Joyce O'Connell was supported by the Department of Defense Breast Cancer Research Predoctoral Traineeship Award (W81XWH-09-1-0008). Dr. Valerie LeBleu was funded from the NIH Research Training Grant in Gastroenterology (2T32DK007760-11). PKM2 antibody was a generous gift from Dr. Matthew Vander Heiden (MIT, Cambridge). I would also like to thank Dr. David Frank, Dr. Lewis Cantley and Dr. Joan Brugge for their advice and helpful discussions.

CHAPTER 5

DISSERTATION SUMMARY

Cells normally use oxidative phosphorylation for efficient energy production and only shift to lactate production under anaerobic conditions. However, cancer cells have adapted to favor lactate production even at normal oxygen levels, exhibiting a metabolic shift known as the Warburg effect. While cancer cells rely on this altered metabolism for rapid proliferation and biosynthesis, the metabolic state of the other cellular constituents within the tumor remains mostly unknown. In breast carcinomas, the stroma comprises of greater than 80% of the tumor mass with fibroblasts being the dominant stromal cell type. Thus, fibroblasts may be important contributors to glucose metabolism in the tumor.

Through comparative studies between cancer-associated fibroblasts (CAFs) and normal mammary fibroblasts (NMFs) of human and mouse origins, we demonstrate that CAFs exhibit the Warburg effect with increased glycolysis and lactate production in aerobic condition with a trend of increased mitochondrial functions and defective antioxidant activity.

We explore two different mechanisms that explain the Warburg effect in fibroblasts. Firstly, methylation studies suggest that enhanced glycolysis in CAFs may be due to epigenetic modifications of regulators of the pathway, fructose-bisphosphatase 1 and pyruvate kinase M2. Secondly, substantial exposure to hypoxia seems to induce prolonged expression of Hif1α via hypomethylation, driving overexpression of its transcriptional targets including glycolysis genes.

To determine the functional contribution of Warburg effect in CAFs, we detail three *in vivo* studies. The first, fibroblast ablation in *αSMA-tk* mouse model, argues that stromal fibroblasts are actively contributing to the glucose metabolism ongoing inside the tumors. Knockdowns of pyruvate dehydrogenase kinase in fibroblasts and knockdown of lactate transporter in cancer cells indicate that not only metabolic status of CAFs affects tumor growth but also suggest that the Warburg effect in CAFs is possibly supporting it.

With all these results, we propose a model to describe the metabolic relationship between CAFs and cancer cells (Figure 21). In the growing tumor, stromal fibroblasts experience an environment full of growth factors, prompting them to proliferate; thus making their glucose metabolism changes to glycolysis and lactate production. As the tumor becomes a substantial mass, CAFs are exposed to direct contact with cancer cells, concentrated level of growth factors, and chronic hypoxia. This tumor progression induces fundamental shifts in expression of *Hif1α* and glycolysis genes such as *Fbp1* and *Pkm2*. These changes allow CAFs to adopt the Warburg effect as a coping mechanism to the tumor microenvironment.

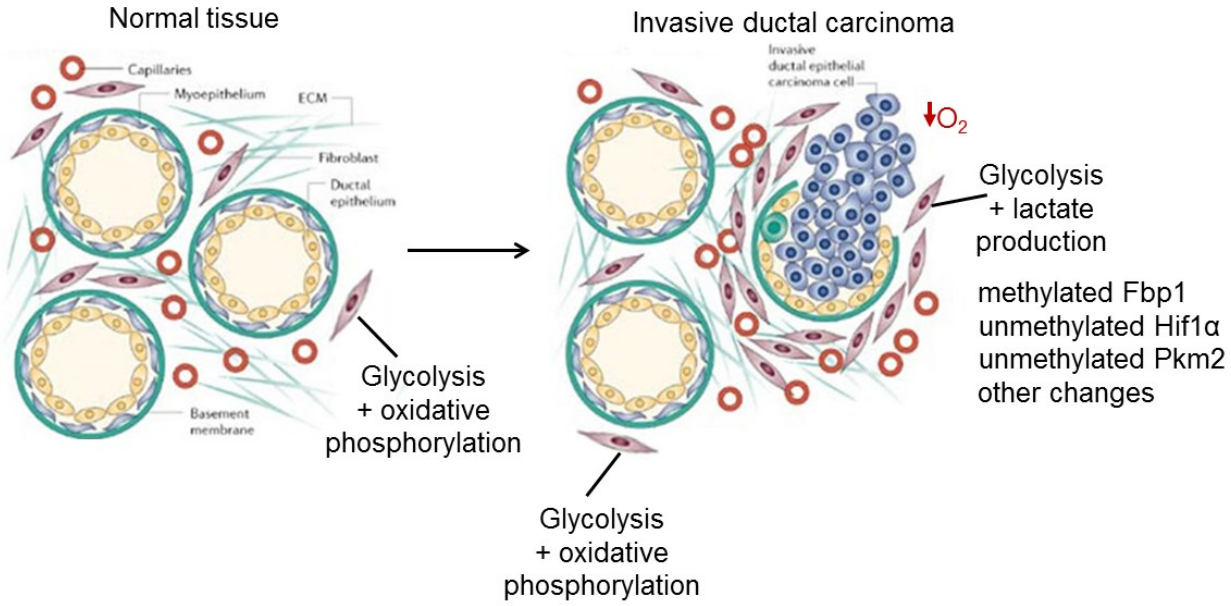

Figure 21. Schematic of metabolic relationship between CAFs and cancer cells.

We also highlight important unanswered questions and framing future directions for the field. Although the presented work uses fibroblasts from breast cancer, we hope to see its expansion to other cancers and relevant diseases. Strong understanding of glucose metabolism in diseased fibroblasts can greatly influence therapeutic strategy and ultimately improve patient care.

MATERIALS AND METHODS

Cell lines

4T1 Balb/c mammary tumor epithelial cells (ATCC) and MEF (Millipore) were grown in Dulbecco's Modified Eagle's Medium supplemented with 10% fetal calf serum and penicillin/streptomycin (each 100U/ml). Human normal mammary fibroblasts and cancer-associated fibroblasts were grown from breast biopsies obtained as part of an institutionally approved clinical study at Boston Brigham and Women's Hospital in collaboration with Dr. Sughra Raza. Mouse normal mammary fibroblasts and cancer-associated fibroblasts were grown from tissues obtained from *αSMA-RFP* mice. Tissues were minced into <1mm^3 pieces and digested overnight with 300U/ml of Collagenase I. Collagenase mixture was replaced with RPMI-1640 media containing 20% fetal calf serum with 100U/ml penicillin/streptomycin and 250ng/ml amphotericin and fibroblasts were allowed to grow out of the tissue pieces. Grown cells underwent FACS to obtain pure αSMA-RFP$^+$ populations.

Transgenic mice

αSMA-RFP and *αSMA-tk* mice were generated by our laboratory using an extended *αSMA* promoter containing approximately 2.4kb of the *αSMA* promoter plus exon 1, intron 1, and part of exon 2 (altogether 5.2kb) amplified with the following primers: 5' CAATGC ATGCTGTACAAACATCAGG 3' (Forward); 5' AGCTGGAGCAGCGTCTCAGGGT TCTGC 3' (Reverse). For the *αSMA-RFP* mice, the extended *αSMA* promoter was cloned into the pDsRed-Express-1 vector (Clontech) using EcoRI and SalI restriction sites, and the whole *αSMA-RFP* construct was released from the vector using EcoRI and DrdI before purification and injection into fertilized eggs. For the *αSMA-tk* mice, a truncated version of the herpes simplex 1 virus thymidine kinase (HSV1-tk) gene with 3' UTR was amplified from

plasmid fsp1-TK using the following primers: 5' ATGCCCACGCTACTGCGGG 3' (Forward); 5' GTGGATAACCGTATTACCGCC 3' (Reverse). The extended *αSMA* promoter was cloned into the pCR2.1-TOPO vector (Invitrogen) using EcoRI and NotI restriction sites, then this *αSMA* promoter-TOPO construct and the *tk* fragment were digested and ligated together. The whole *αSMA-tk* construct was released from the vector using EcoRI and XbaI then purified and injected into fertilized eggs. All transgenic mice were created in the Brigham and Women's Hospital Transgenic Core Facility on a FVB background and backcrossed more than 7 generations to a BALB/c background for experiments. Mice were generated by Dr. Yingqi Teng and Dr. Joyce O'Connell (BIDMC and Harvard Medical School, Boston).

Generation of knockdowns

MEF clones containing knockdown of *Pdk* were made following the Addgene protocol using pLKO.1 – TRC cloning vector with help from Dr. Valerie LeBleu. shRNA oligos were 5' CCGGGAACTCCGACCAGAAGCCAAGAATTCTCGAGAATTCTTGGCTTCTGGTCGGAGT TCTTTTTG 3' (Forward) and 5' AATTCAAAAAGAACTCCGACCAGAAGCCAAGAATTCT CGAGAATTCTTGGCTTCTGGTCGGAGTTC 3' (Reverse). Target sequence was 5' GAACTCCGACCAGAAGCCAAGAATT 3'. Control scrambled shRNA oligos were 5' CCGGGAACACGTCAGACCAGGATCACATACTCGAGTATGTGATCCTGGTCTGACGTGT TCTTTTTG 3' (Forward) and 5' AATTCAAAAAGAACACGTCAGACCAGGATCACATACT CGAGTATGTGATCCTGGTCTGACGTGTTC 3' (Reverse) with target sequence being 5' GAACACGTCAGACCAGGATCACATA 3'.

4T1 clones containing knockdown of *Mct1* were made by transfecting shRNA (Origene) in Lipofectamine lipid carrier (Invitrogen) using standard transfection protocol. Clone selection with 4ug/ml puromycin was done prior to clone picking and verification of gene knockdown was confirmed with qRT-PCR. Scrambled shRNA (Origene) was control.

Cancer cell implantation

Female BALB/c mice were used for orthotopic mammary fat pad injection of 4T1 mouse mammary carcinoma cells. $1x10^6$ tumor cells were injected into the mammary fat pad in 20µl of PBS (with help from Dr. Joyce O'Connell); mice were sacrificed 24 days post cancer cell implantation. *αSMA-tk* mice experiment was from Tse (2011). Briefly, mice received daily intraperitoneal injections with 50mg/kg of ganciclovir starting 12 days post cancer cell implantation. MEF were mixed with 4T1 cells at a 2:1 ratio for orthotopic implantation into the mammary fat pad, and mice were sacrificed 21 days post cancer cell implantation. Tumor volumes were measured using Vernier calipers and volumes were calculated using a standard formula (length x width^2 x 0.52). Age-matched mice were used for all studies. Mouse studies followed the Institutional Animal Care and Use Guidelines at the BIDMC.

Fluorescence-activated cell sorting

Fluorescence-activated cell sorting (FACS) was performed on single cell suspensions. Tissues were chopped finely then incubated in 1mg/ml collagenase/dispase solution (Roche) for 1 hour in a 37°C shaker. The resulting suspension was filtered through a 40µm cell strainer, treated with ACK lysis buffer for removal of red blood cells and resuspended in PBS sorting solution of 2% FBS in plus propidium iodide. Cultured cells were trypsinized and pelleted before filtering and resuspension in sorting solution and sorted at Joslin Flow Cytometry Core Facility.

Microarray

For tumors and human fibroblasts, RNAs were extracted with TRIzol (Invitrogen) per manufacturer's instructions. For mouse fibroblasts, αSMA-RFP$^+$ stromal cells were isolated by fluorescence-activated cell sorting (FACS) from normal breast tissues and tumors. RNA was extracted immediately using the Qiagen RNeasy Plus Micro Kit per manufacturer's instructions, then amplified with the NuGen WT-Ovation Pico Kit (done by Dr. Joyce O'Connell). Microarray hybridization to the Human HT-12 Expression BeadChip or the Mouse Ref-8 Expression BeadChip (Illumina) was performed by the Molecular Genetics Core Facility at Children's Hospital Boston. The Ingenuity Pathways Analysis software was used for comparative gene expression with help from Dr. Joyce O'Connell.

Quantitative real time PCR

Primers were used with SYBR Green PCR Master Mix in a 7300 Sequence Detector System (Applied Biosystems) and measurements were standardized to expression of the housekeeping genes, either acidic ribosomal phosphoprotein PO (ARP/ 36B4) or β-actin. Fold-change in gene expression was determined using the ΔΔCt method. For primer sequences, see below.

Table 3. qRT-PCR primer sequences.

Gene	Species	Primer sequences
Glut1	M. Musculus	F 5' AGTGTATCCTGTTGCCCTTCT 3' R 5' CATCGGCTGTCCCTCGAAGC 3'
	H. Sapien	F 5' AAGGTGATCGAGGAGTTCTACA 3' R 5' ATGCCCCCAACAGAAAAGATG 3'
Hk2	M. Musculus	F 5' GGAACCGCCTAGAAATCTCC 3' R 5' GGAGCTCAACCAAAACCAAG 3'
	H. Sapien	F 5' TTTGACCACATTGCCGAATGC 3' R 5' GGTCCATGAGACCAGGAAACT 3'

Table 3 (continued)

Gene	Species	Primer sequences
LdhA	M. Musculus	F 5’ TGGAGTGGAATGAATGTTGC 3’ R 5’ ATAGCCCAGGATGTGTAGCC 3’
	H. Sapien	F 5' CAGCCCGAACTGCAAGTTG 3' R 5' CCCCCATCAGGTAACGGAATC 3'
Pkm2	M. Musculus	F 5’ GCCGCCTGGACATTGACTC 3’ R 5’ CCATGAGAGAAATTCAGCCGAG 3’
	H. Sapien	F 5’ ATGTCGAAGCCCGATAGTGAA 3’ R 5’ TGGGTGGTGAATCAATGTCCA 3’
Pfkl	M. Musculus	F 5’ CCCTGACAGCAGCATTCATA 3’ R 5’ CTACCGTGGACCTGGAGAAA 3’
	H. Sapien	F 5’ GCTGGGCGGCACTATCATT 3’ R 5’ TCAGGTGCGAGTAGGTCCG 3’
Mct4	M. Musculus	F 5' GGGGCCTACTGCTCAACTG 3' R 5' CGGTCTCGGAAGACACTCAG 3'
	H. Sapien	F 5' TGACTGGACAGGTATCCTTGAG 3' R 5' AGTAGTGGAAATGTGGTGGCTA 3'
Mct1	M. Musculus	F 5' TGTTAGTCGGAGCCTTCATTTC 3' R 5' CACTGGTCGTTGCACTGAATA 3'
Hif1α	H. Sapien	F 5' CTGCCACCACTGATGAATTA 3' F 5' GTATGTGGGTAGGAGATGGA 3'
Pdk1	M. Musculus	F 5’ TTACTCAGTGGAACACCGCC 3’ R 5’ GTTTATCCCCCGATTCAGGT 3’
Pdk2	M. Musculus	F 5’ AGGGGCACCCAAGTACATC 3’ R 5’ TGCCGGAGGAAAGTGAATGAC 3’
Pdk3	M. Musculus	F 5’ TCCTGGACTTCGGAAGGGATA 3’ R 5’ GAAGGGCGGTTCAACAAGTTA 3’
Pdk4	M. Musculus	F 5’ CTTCTGGGCTCTTCTCATGG 3’ R 5’ GATTGACATCCTGCCTGACC 3’
Fbp1	H. Sapien	F 5' CTACGCCAGGGACTTTGACC 3' R 5' GGCCCCATAAGGAGCTGAAT 3'
Arp/36b4	M. Musculus	F 5’ GGAGCCAGCGAGGCCACACTGCTG 3’ R 5’ CTGGCCACGTTGCGGACACCCTCC 3’
β-actin	H. Sapien	F 5' CATGTACGTTGCTATCCAGGC 3' R 5' CTCCTTAATGTCACGCACGAT 3'

Metabolomics

Metabolomics was done with targeted mass spectrometry through collaboration with Dr. John Asara (BIDMC, Boston). For cultured cells, 4ml of 80% LC-MS grade methanol was added to each 10cm dish and incubated at -80°C for 15 minutes. Cells were scraped and collected from plate to be centrifuged at full speed for 5 minutes at 4°C to pellet cell debris and proteins. Supernatants were saved. Pellets were resuspended in 500µl 80% methanol by vortexing and subsequently centrifuged as before. Supernatant was collected and pellet resuspension was repeated. The three extracted supernatants were pooled for drying step. For tissues, 400ml of 80% LC-MS grade methanol was added per 1-2mg weight and homogenized for 30 seconds at -80°C then centrifuged at 14,000rpm for 10 minutes at 4°C. Supernatants were collected and the steps from the beginning were repeated twice. Supernatants from all three extractions were pooled and centrifuged a final time at 14,000rpm for 10 minutes at 4°C. For FACS cells, 400-500µl 80% methanol was used per sample and the above described subsequent steps were followed. Metabolite supernatants were dried by SpeedVac. Samples were re-suspended using 20µL HPLC grade water for mass spectrometry. A total of 299 endogenous water soluble metabolites including some in both positive and negative ion mode were analyzed by a 5500 QTRAP triple quadrupole mass spectrometer (AB/Sciex) coupled to a Prominence UFLC HPLC system (Shimadzu) via selected reaction monitoring (SRM). Metabolomics data analysis was done using Metaboanalyst software (www.metaboanalsyst.ca) with the following settings: 1) automatic removal of variables with >50% missing values, 2) calculation of the remaining missing values as half of the minimum positive value in the original data, and 3) autoscaling for column-wise normalization. Relative metabolite abundance for each metabolite was calculated and graphed in log2 scale (done with help from Dr. Joyce O'Connell).

Quantification of lactate

L-Lactate Assay Kit was purchased from Eton Bioscience Inc. and used per manufacturer's instructions. Cells were plated at the same number and volume. Culture mediums were collected 72 hours later and were diluted 1:10 with ddH2O prior to adding assay solution. Concentrations of lactate in samples were determined with the standard curve. Cell numbers counted at the time of medium harvest were used for normalization. Relative ratio of CAFs to NMFs was calculated and graphed.

Assessments of mitochondrial functions

Cells were plated in triplicate at 4x10^4 cells/well into XF24 plate for 24 hours prior to assay with XF Cell Mito Stress Kit using the XF24 Analyzer plate reader (in collaboration with Karina Gonzales and Dr. Marcia Haigis, Harvard Medical School, Boston). Rotenone was used at 1uM final concentration to obtain mitochondrial-specific OCR. All products were obtained from Seahorse Bioscience. Gathered OCR, PPR and ECAR data were normalized to cell number (crystal violet) and relative rates were calculated for comparison. Activities of complexes I, II and IV of the electron transport chain were determined by level of NADH, fumarate/succinate and ATP/ADP ratios respectively (quantification done by metabolomics). Relative activities were calculated for comparison. mtDNA contents were measured on whole cell DNA extracts by qRT-PCR (done by Dr. Joyce O'Connell) with the following sequences:

Cyba F 5' CCCAGTGGTACTTTGGTGCC 3'

R 5' GCGGTCATGTACTTCTGTCCC 3'

β-Globin F 5' AGGAGAAGTCTGCCGTTACTG 3'

R 5' CCGAGCACTTTCTTGCCATGA 3'

Immunoblotting

Homogenized tissues and cells were lysed with RIPA buffer using standard protocol. Protein concentrations were determined by BCA Protein Assay (Thermo Scientific) with a microplate reader at 562nm. Lysates were run on 10% polyacrylamide gels and proteins transferred onto PVDF membranes overnight. Membranes were blocked with 5% milk in TBS-T. Antibodies detecting GLUT1 (Abcam), HK2 (Cell Signaling), LDHA (Cell Signaling), β-ACTIN (Sigma), MCT1 (Santa Cruz), MCT4 (Santa Cruz), HIF1α (Novus Biologicals), β-TUBULIN (Abcam) and PKM2 (generously provided by Dr. Matthew Vander Heiden) were used at recommended dilutions for either 4 hours at room temperature or overnight at 4°C on shaker. Appropriate HRP-conjugated secondary antibodies (Sigma) were used at 1:10,000 dilution for one hour at room temperature on shaker. Membranes were exposed to ECL solution (Thermo Scientific) prior to film exposure.

Methylation studies

Genomic DNAs were isolated using high salt precipitation protocol and subsequently purified. Next, high throughput methylation specific oligonucleotide microarray was performed (~27,500 CpG islands with ~485,000 probes) in collaboration with Dr. Manuel Esteller (IDIBELL, Spain). Percent methylation data and heat map were generated by Javier Carmona Sanz (IDIBELL, Spain) and differential % of methylation for each probe was calculated to compare CAF to NMF.

Methylated DNA immunoprecipitation followed by SYBR-based real time PCR (in collaboration with Dr. Desiree Tampe and Dr. Michael Zeisberg (University Hospital Goettingen, Germany) was completed for *Fbp1*, *Pkm2* and *Hif1α*. PCR band intensities

were quantified and average %MeDIP/input DNA were calculated. In addition, bisulfite sequencing of *Fbp1* was also performed (IDIBELL, Spain).

Primer sequences

Fbp1 F 5' CGAGCGCTGCGGACACTCGGG 3'

R 5' CGCACCGCCGAAGAGATGGC 3'

Pkm2 F 5' CTACTCTGAGGCATTCGCTCTGC 3'

R 5' CCGGGTGTCTGCTCTGGCGCAC 3'

Hif1α F 5' GGAGAAAGAGAGCAGGAGCATTAC 3'

R 5' GCTCGTCTGTGTTTAGCGGCGGAGG 3'

Statistical analysis

For comparison between two groups, a two-tailed *t*-test was performed. P-value <0.05 constitutes statistical significance.

REFERENCES

Allinen, M., Beroukhim, R., Cai, L., Brennan, C., Lahti-Domenici, J., Huang, H., … Polyak, K. (2004). Molecular characterization of the tumor microenvironment in breast cancer. *Cancer cell*, *6*(1), 17–32. doi:10.1016/j.ccr.2004.06.010

Balliet, R. M., Capparelli, C., Guido, C., Pestell, T. G., Martinez-Outschoorn, U. E., Lin, Z., … Lisanti, M. P. (2011). Mitochondrial oxidative stress in cancer-associated fibroblasts drives lactate production, promoting breast cancer tumor growth: understanding the aging and cancer connection. *Cell cycle (Georgetown, Tex.)*, *10*(23), 4065–4073. doi:10.4161/cc.10.23.18254

Bigl, M., Jandrig, B., Horn, L.-C., & Eschrich, K. (2008). Aberrant methylation of human L- and M-fructose 1,6-bisphosphatase genes in cancer. Biochemical and biophysical research communications, 377(2), 720–724. doi:10.1016/j.bbrc.2008.10.045

Biochem.co. Glycolysis. Retrieved 3/2013 from http://biochem.co/2010/02/glycolysis/. 2010

Bissell, M. J., & Radisky, D. (2001). Putting tumours in context. Nature reviews. Cancer, 1(1), 46–54. doi:10.1038/35094059

Bisson, C., Blacher, S., Polette, M., Blanc, J.-F., Kebers, F., Desreux, J., … Noel, A. (2003). Restricted expression of membrane type 1-matrix metalloproteinase by myofibroblasts adjacent to human breast cancer cells. International journal of cancer. Journal international du cancer, 105(1), 7–13. doi:10.1002/ijc.11012

Bonnet, S., Archer, S. L., Allalunis-Turner, J., Haromy, A., Beaulieu, C., Thompson, R., … Michelakis, E. D. (2007). A mitochondria-K+ channel axis is suppressed in cancer and its normalization promotes apoptosis and inhibits cancer growth. Cancer cell, 11(1), 37–51. doi:10.1016/j.ccr.2006.10.020

Bonuccelli, G., Whitaker-Menezes, D., Castello-Cros, R., Pavlides, S., Pestell, R. G., Fatatis, A., … Lisanti, M. P. (2010). The reverse Warburg effect: glycolysis inhibitors prevent the tumor promoting effects of caveolin-1 deficient cancer associated fibroblasts. Cell cycle (Georgetown, Tex.), 9(10), 1960–1971.

Brown, J. M., & Wilson, W. R. (2004). Exploiting tumour hypoxia in cancer treatment. Nature reviews. Cancer, 4(6), 437–447. doi:10.1038/nrc1367

Breastcancer.org. U.S. Breast cancer statistics. Retrieved 5/15/2012 from http://www.breastcancer.org/symptoms/understand_bc/statistics. 2012

Campbell, I. G., Qiu, W., Polyak, K., & Haviv, I. (2008). Breast-cancer stromal cells with TP53 mutations. The New England journal of medicine, 358(15), 1634–1635; author reply 1636. doi:10.1056/NEJMc086024

Centers for Disease Control and Prevention. Cancer Prevention and Control. Retrieved 1/30/2011 from http://www.cdc.gov/cancer/dcpc/data/women.htm. 2010

Chiaradonna, F., Gaglio, D., Vanoni, M., & Alberghina, L. (2006). Expression of transforming K-Ras oncogene affects mitochondrial function and morphology in mouse fibroblasts. Biochimica et biophysica acta, 1757(9-10), 1338–1356. doi:10.1016/j.bbabio.2006.08.001

Christofk, H. R., Vander Heiden, M. G., Harris, M. H., Ramanathan, A., Gerszten, R. E., Wei, R., … Cantley, L. C. (2008). The M2 splice isoform of pyruvate kinase is important for cancer metabolism and tumour growth. Nature, 452(7184), 230–233. doi:10.1038/nature06734

Couet, J., Sargiacomo, M., & Lisanti, M. P. (1997). Interaction of a receptor tyrosine kinase, EGF-R, with caveolins. Caveolin binding negatively regulates tyrosine and serine/threonine kinase activities. The Journal of biological chemistry, 272(48), 30429–30438.

Crawford, Y., Kasman, I., Yu, L., Zhong, C., Wu, X., Modrusan, Z., … Ferrara, N. (2009). PDGF-C mediates the angiogenic and tumorigenic properties of fibroblasts associated with tumors refractory to anti-VEGF treatment. Cancer cell, 15(1), 21–34. doi:10.1016/j.ccr.2008.12.004

Denko, N. C. (2008). Hypoxia, HIF1 and glucose metabolism in the solid tumour. Nature reviews. Cancer, 8(9), 705–713. doi:10.1038/nrc2468

Dong, J., Grunstein, J., Tejada, M., Peale, F., Frantz, G., Liang, W.-C., … Ferrara, N. (2004). VEGF-null cells require PDGFR alpha signaling-mediated stromal fibroblast recruitment for tumorigenesis. The EMBO journal, 23(14), 2800–2810. doi:10.1038/sj.emboj.7600289

Dvorak, H. F. (1986). Tumors: wounds that do not heal. Similarities between tumor stroma generation and wound healing. The New England journal of medicine, 315(26), 1650–1659. doi:10.1056/NEJM198612253152606

Ebert, B. L., Firth, J. D., & Ratcliffe, P. J. (1995). Hypoxia and mitochondrial inhibitors regulate expression of glucose transporter-1 via distinct Cis-acting sequences. The Journal of biological chemistry, 270(49), 29083–29089.

Fang, J., Yan, L., Shing, Y., & Moses, M. A. (2001). HIF-1alpha-mediated up-regulation of vascular endothelial growth factor, independent of basic fibroblast growth factor, is important in the switch to the angiogenic phenotype during early tumorigenesis. Cancer research, 61(15), 5731–5735.

Fiaschi, T., Marini, A., Giannoni, E., Taddei, M. L., Gandellini, P., De Donatis, A., … Chiarugi, P. (2012). Reciprocal metabolic reprogramming through lactate shuttle coordinately influences tumor-stroma interplay. Cancer research, 72(19), 5130–5140. doi:10.1158/0008-5472.CAN-12-1949

Fiegl, H., Millinger, S., Goebel, G., Müller-Holzner, E., Marth, C., Laird, P. W., & Widschwendter, M. (2006). Breast cancer DNA methylation profiles in cancer cells and tumor stroma: association with HER-2/neu status in primary breast cancer. Cancer research, 66(1), 29–33. doi:10.1158/0008-5472.CAN-05-2508

Firth, J. D., Ebert, B. L., & Ratcliffe, P. J. (1995). Hypoxic regulation of lactate dehydrogenase A. Interaction between hypoxia-inducible factor 1 and cAMP response elements. The Journal of biological chemistry, 270(36), 21021–21027.

Forouzanfar, M. H., Foreman, K. J., Delossantos, A. M., Lozano, R., Lopez, A. D., Murray, C. J. L., & Naghavi, M. (2011). Breast and cervical cancer in 187 countries between 1980 and 2010: a systematic analysis. Lancet, 378(9801), 1461–1484. doi:10.1016/S0140-6736(11)61351-2

Fritz, V., & Fajas, L. (2010). Metabolism and proliferation share common regulatory pathways in cancer cells. Oncogene, 29(31), 4369–4377. doi:10.1038/onc.2010.182

Fulda, S., Galluzzi, L., & Kroemer, G. (2010). Targeting mitochondria for cancer therapy. Nature reviews. Drug discovery, 9(6), 447–464. doi:10.1038/nrd3137

Gabbiani, G. (1992). The biology of the myofibroblast. Kidney international, 41(3), 530–532.

Goel, A., Mathupala, S. P., & Pedersen, P. L. (2003). Glucose metabolism in cancer. Evidence that demethylation events play a role in activating type II hexokinase gene expression. The Journal of biological chemistry, 278(17), 15333–15340. doi:10.1074/jbc.M300608200

Harris, A. L. (2002). Hypoxia--a key regulatory factor in tumour growth. Nature reviews. Cancer, 2(1), 38–47. doi:10.1038/nrc704

Hawsawi, N. M., Ghebeh, H., Hendrayani, S.-F., Tulbah, A., Al-Eid, M., Al-Tweigeri, T., … Aboussekhra, A. (2008). Breast carcinoma-associated fibroblasts and their counterparts display neoplastic-specific changes. Cancer research, 68(8), 2717–2725. doi:10.1158/0008-5472.CAN-08-0192

Hinz, B., Phan, S. H., Thannickal, V. J., Galli, A., Bochaton-Piallat, M.-L., & Gabbiani, G. (2007). The myofibroblast: one function, multiple origins. The American journal of pathology, 170(6), 1807–1816. doi:10.2353/ajpath.2007.070112

Hlatky, L., Tsionou, C., Hahnfeldt, P., & Coleman, C. N. (1994). Mammary fibroblasts may influence breast tumor angiogenesis via hypoxia-induced vascular endothelial growth factor up-regulation and protein expression. Cancer research, 54(23), 6083–6086.

Hosein, A. N., Wu, M., Arcand, S. L., Lavallée, S., Hébert, J., Tonin, P. N., & Basik, M. (2010). Breast carcinoma-associated fibroblasts rarely contain p53 mutations or chromosomal aberrations. Cancer research, 70(14), 5770–5777. doi:10.1158/0008-5472.CAN-10-0673

Hu, M., & Polyak, K. (2008). Molecular characterisation of the tumour microenvironment in breast cancer. European journal of cancer (Oxford, England: 1990), 44(18), 2760–2765. doi:10.1016/j.ejca.2008.09.038

Hu, M., Yao, J., Cai, L., Bachman, K. E., Van den Brûle, F., Velculescu, V., & Polyak, K. (2005). Distinct epigenetic changes in the stromal cells of breast cancers. Nature

genetics, 37(8), 899–905. doi:10.1038/ng1596

Isidoro, A., Casado, E., Redondo, A., Acebo, P., Espinosa, E., Alonso, A. M., … Cuezva, J. M. (2005). Breast carcinomas fulfill the Warburg hypothesis and provide metabolic markers of cancer prognosis. Carcinogenesis, 26(12), 2095–2104. doi:10.1093/carcin/bgi188

Iyer, N. V., Kotch, L. E., Agani, F., Leung, S. W., Laughner, E., Wenger, R. H., … Semenza, G. L. (1998). Cellular and developmental control of O2 homeostasis by hypoxia-inducible factor 1 alpha. Genes & development, 12(2), 149–162.

Jiang, L., Gonda, T. A., Gamble, M. V., Salas, M., Seshan, V., Tu, S., … Tycko, B. (2008). Global hypomethylation of genomic DNA in cancer-associated myofibroblasts. Cancer research, 68(23), 9900–9908. doi:10.1158/0008-5472.CAN-08-1319

Jones, R. G., & Thompson, C. B. (2009). Tumor suppressors and cell metabolism: a recipe for cancer growth. Genes & development, 23(5), 537–548. doi:10.1101/gad.1756509

Kallinowski, F., Schlenger, K. H., Runkel, S., Kloes, M., Stohrer, M., Okunieff, P., & Vaupel, P. (1989). Blood flow, metabolism, cellular microenvironment, and growth rate of human tumor xenografts. Cancer research, 49(14), 3759–3764.

Kalluri, R., & Zeisberg, M. (2006). Fibroblasts in cancer. Nature reviews. Cancer, 6(5), 392–401. doi:10.1038/nrc1877

Kim, J., Tchernyshyov, I., Semenza, G. L., & Dang, C. V. (2006). HIF-1-mediated expression of pyruvate dehydrogenase kinase: a metabolic switch required for cellular adaptation to hypoxia. Cell metabolism, 3(3), 177–185. doi:10.1016/j.cmet.2006.02.002

Koukourakis, M. I., Giatromanolaki, A., Harris, A. L., & Sivridis, E. (2006). Comparison of metabolic pathways between cancer cells and stromal cells in colorectal carcinomas: a metabolic survival role for tumor-associated stroma. Cancer research, 66(2), 632–637. doi:10.1158/0008-5472.CAN-05-3260

Kuperwasser, C., Chavarria, T., Wu, M., Magrane, G., Gray, J. W., Carey, L., … Weinberg, R. A. (2004). Reconstruction of functionally normal and malignant human breast tissues in mice. Proceedings of the National Academy of Sciences of the United States of America, 101(14), 4966–4971. doi:10.1073/pnas.0401064101

Lajoie, P., & Nabi, I. R. (2010). Lipid rafts, caveolae, and their endocytosis. International review of cell and molecular biology, 282, 135–163. doi:10.1016/S1937-6448(10)82003-9

Lehninger, Albert, David Nelson, and Michael Cox. Principles of Biochemistry. 4. W.H. Freeman, 2004

Liu, X., Wang, X., Zhang, J., Lam, E. K. Y., Shin, V. Y., Cheng, A. S. L., … Jin, H. C. (2010). Warburg effect revisited: an epigenetic link between glycolysis and gastric carcinogenesis. Oncogene, 29(3), 442–450. doi:10.1038/onc.2009.332

MacDougall, J. R., & Matrisian, L. M. (1995). Contributions of tumor and stromal matrix metalloproteinases to tumor progression, invasion and metastasis. Cancer metastasis reviews, 14(4), 351–362.

Mercier, I., Casimiro, M. C., Wang, C., Rosenberg, A. L., Quong, J., Minkeu, A., … Lisanti, M. P. (2008). Human breast cancer-associated fibroblasts (CAFs) show caveolin-1 downregulation and RB tumor suppressor functional inactivation: Implications for the response to hormonal therapy. Cancer biology & therapy, 7(8), 1212–1225.

Michelakis, E. D., Sutendra, G., Dromparis, P., Webster, L., Haromy, A., Niven, E., … Petruk, K. C. (2010). Metabolic modulation of glioblastoma with dichloroacetate. Science translational medicine, 2(31), 31ra34. doi:10.1126/scitranslmed.3000677

Migneco, G., Whitaker-Menezes, D., Chiavarina, B., Castello-Cros, R., Pavlides, S., Pestell, R. G., … Lisanti, M. P. (2010). Glycolysis cancer associated fibroblasts promote breast cancer tumor growth, without a measurable increase in angiogenesis: evidence for stromal-epithelial metabolic coupling. Cell cycle (Georgetown, Tex.), 9(12), 2412–2422.

Olumi, A. F., Grossfeld, G. D., Hayward, S. W., Carroll, P. R., Tlsty, T. D., & Cunha, G. R. (1999). Carcinoma-associated fibroblasts direct tumor progression of initiated human prostatic epithelium. Cancer research, 59(19), 5002–5011.

Orimo, A, Tomioka, Y., Shimizu, Y., Sato, M., Oigawa, S., Kamata, K., … Muramatsu, M. (2001). Cancer-associated myofibroblasts possess various factors to promote endometrial tumor progression. Clinical cancer research: an official journal of the American Association for Cancer Research, 7(10), 3097–3105.

Orimo, Akira, Gupta, P. B., Sgroi, D. C., Arenzana-Seisdedos, F., Delaunay, T., Naeem, R., … Weinberg, R. A. (2005). Stromal fibroblasts present in invasive human breast carcinomas promote tumor growth and angiogenesis through elevated SDF-1/CXCL12 secretion. Cell, 121(3), 335–348. doi:10.1016/j.cell.2005.02.034

Papandreou, I., Cairns, R. A., Fontana, L., Lim, A. L., & Denko, N. C. (2006). HIF-1 mediates adaptation to hypoxia by actively downregulating mitochondrial oxygen consumption. Cell metabolism, 3(3), 187–197. doi:10.1016/j.cmet.2006.01.012

Patocs, A., Zhang, L., Xu, Y., Weber, F., Caldes, T., Mutter, G. L., … Eng, C. (2007). Breast-cancer stromal cells with TP53 mutations and nodal metastases. The New England journal of medicine, 357(25), 2543–2551. doi:10.1056/NEJMoa071825

Pavlides, S., Whitaker-Menezes, D., Castello-Cros, R., Flomenberg, N., Witkiewicz, A. K., Frank, P. G., … Lisanti, M. P. (2009). The reverse Warburg effect: aerobic glycolysis in cancer associated fibroblasts and the tumor stroma. Cell cycle (Georgetown, Tex.), 8(23), 3984–4001.

Pennsylvania State University Libraries. APA Citation Guide. Retrieved 3/2013 from http://www.libraries.psu.edu/psul/lls/students/intext.html. 2013

Polyak, K., & Kalluri, R. (2010). The role of the microenvironment in mammary gland

development and cancer. Cold Spring Harbor perspectives in biology, 2(11), a003244. doi:10.1101/cshperspect.a003244

Pouysségur, J., Dayan, F., & Mazure, N. M. (2006). Hypoxia signalling in cancer and approaches to enforce tumour regression. Nature, 441(7092), 437–443. doi:10.1038/nature04871

Qiu, W., Hu, M., Sridhar, A., Opeskin, K., Fox, S., Shipitsin, M., … Campbell, I. G. (2008). No evidence of clonal somatic genetic alterations in cancer-associated fibroblasts from human breast and ovarian carcinomas. Nature genetics, 40(5), 650–655. doi:10.1038/ng.117

Razani, B., Zhang, X. L., Bitzer, M., Von Gersdorff, G., Böttinger, E. P., & Lisanti, M. P. (2001). Caveolin-1 regulates transforming growth factor (TGF)-beta/SMAD signaling through an interaction with the TGF-beta type I receptor. The Journal of biological chemistry, 276(9), 6727–6738. doi:10.1074/jbc.M008340200

Rozenchan, P. B., Carraro, D. M., Brentani, H., De Carvalho Mota, L. D., Bastos, E. P., E Ferreira, E. N., … Brentani, M. M. (2009). Reciprocal changes in gene expression profiles of cocultured breast epithelial cells and primary fibroblasts. International journal of cancer. Journal international du cancer, 125(12), 2767–2777. doi:10.1002/ijc.24646

Schmitt-Gräff, A., Desmoulière, A., & Gabbiani, G. (1994). Heterogeneity of myofibroblast phenotypic features: an example of fibroblastic cell plasticity. Virchows Archiv: an international journal of pathology, 425(1), 3–24.

Semenza, G L. (2010). Defining the role of hypoxia-inducible factor 1 in cancer biology and therapeutics. Oncogene, 29(5), 625–634. doi:10.1038/onc.2009.441

Semenza, G L, Jiang, B. H., Leung, S. W., Passantino, R., Concordet, J. P., Maire, P., & Giallongo, A. (1996). Hypoxia response elements in the aldolase A, enolase 1, and lactate dehydrogenase A gene promoters contain essential binding sites for hypoxia-inducible factor 1. The Journal of biological chemistry, 271(51), 32529–32537.

Semenza, G L, Roth, P. H., Fang, H. M., & Wang, G. L. (1994). Transcriptional regulation of genes encoding glycolysis enzymes by hypoxia-inducible factor 1. The Journal of biological chemistry, 269(38), 23757–23763.

Semenza, Gregg L. (2010). HIF-1: upstream and downstream of cancer metabolism. Current opinion in genetics & development, 20(1), 51–56. doi:10.1016/j.gde.2009.10.009

Seyfried, T. N., & Shelton, L. M. (2010). Cancer as a metabolic disease. Nutrition & metabolism, 7, 7. doi:10.1186/1743-7075-7-7

Shackelford, D. B., & Shaw, R. J. (2009). The LKB1-AMPK pathway: metabolism and growth control in tumour suppression. Nature reviews. Cancer, 9(8), 563–575. doi:10.1038/nrc2676

Shahrzad, S., Bertrand, K., Minhas, K., & Coomber, B. L. (2007). Induction of DNA hypomethylation by tumor hypoxia. Epigenetics: official journal of the DNA Methylation Society, 2(2), 119–125.

Shimoda, M., Mellody, K. T., & Orimo, A. (2010). Carcinoma-associated fibroblasts are a rate-limiting determinant for tumour progression. Seminars in cell & developmental biology, 21(1), 19–25. doi:10.1016/j.semcdb.2009.10.002

Silzle, T., Kreutz, M., Dobler, M. A., Brockhoff, G., Knuechel, R., & Kunz-Schughart, L. A. (2003). Tumor-associated fibroblasts recruit blood monocytes into tumor tissue. European journal of immunology, 33(5), 1311–1320. doi:10.1002/eji.200323057

Skalli, O., Schürch, W., Seemayer, T., Lagacé, R., Montandon, D., Pittet, B., & Gabbiani, G. (1989). Myofibroblasts from diverse pathologic settings are heterogeneous in their content of actin isoforms and intermediate filament proteins. Laboratory investigation; a journal of technical methods and pathology, 60(2), 275–285.

Skobe, M., & Fusenig, N. E. (1998). Tumorigenic conversion of immortal human keratinocytes through stromal cell activation. Proceedings of the National Academy of Sciences of the United States of America, 95(3), 1050–1055.

Sonveaux, P., Végran, F., Schroeder, T., Wergin, M. C., Verrax, J., Rabbani, Z. N., … Dewhirst, M. W. (2008). Targeting lactate-fueled respiration selectively kills hypoxic tumor cells in mice. The Journal of clinical investigation, 118(12), 3930–3942. doi:10.1172/JCI36843

Sugimoto, H., Mundel, T. M., Kieran, M. W., & Kalluri, R. (2006). Identification of fibroblast heterogeneity in the tumor microenvironment. Cancer biology & therapy, 5(12), 1640–1646.

Sun, R. C., Fadia, M., Dahlstrom, J. E., Parish, C. R., Board, P. G., & Blackburn, A. C. (2010). Reversal of the glycolysis phenotype by dichloroacetate inhibits metastatic breast cancer cell growth in vitro and in vivo. Breast cancer research and treatment, 120(1), 253–260. doi:10.1007/s10549-009-0435-9

Surowiak, P., Murawa, D., Materna, V., Maciejczyk, A., Pudelko, M., Ciesla, S., … Lage, H. (2007). Occurence of stromal myofibroblasts in the invasive ductal breast cancer tissue is an unfavourable prognostic factor. Anticancer research, 27(4C), 2917–2924.

Susan G. Komen for the Cure. Breast Cancer Statistics. Retrieved 5/30/2012 from http://ww5.komen.org/breastcancer/statistics.html. 2012

Tlsty, T. D., & Hein, P. W. (2001). Know thy neighbor: stromal cells can contribute oncogenic signals. Current opinion in genetics & development, 11(1), 54–59.

Tse J. (2011). Functional heterogeneity of fibroblasts in cancer progression and metastasis (Doctoral Dissertation). Retrieved 3/2013 from ProQuest Dissertation and Theses database. (UMI No. 3462148)

Tseng, L.-M., Yin, P.-H., Chi, C.-W., Hsu, C.-Y., Wu, C.-W., Lee, L.-M., … Lee, H.-C. (2006). Mitochondrial DNA mutations and mitochondrial DNA depletion in breast cancer. Genes, chromosomes & cancer, 45(7), 629–638. doi:10.1002/gcc.20326

Tuxhorn, J. A., McAlhany, S. J., Dang, T. D., Ayala, G. E., & Rowley, D. R. (2002). Stromal cells promote angiogenesis and growth of human prostate tumors in a differential reactive stroma (DRS) xenograft model. Cancer research, 62(11), 3298–3307.

Vander Heiden, M. G., Cantley, L. C., & Thompson, C. B. (2009). Understanding the Warburg effect: the metabolic requirements of cell proliferation. Science (New York, N.Y.), 324(5930), 1029–1033. doi:10.1126/science.1160809

Vaupel, P., Fortmeyer, H. P., Runkel, S., & Kallinowski, F. (1987). Blood flow, oxygen consumption, and tissue oxygenation of human breast cancer xenografts in nude rats. Cancer research, 47(13), 3496–3503.

Warburg, O., Posener, K., Negelein, E. (1930). Ueber den Stoffwechsel der Tumoren; Biochemische Zeitschrift, Vol. 152, pp. 319-344, 1924. (German). Reprinted in English in the book On metabolism of tumors by O. Warburg, Publisher: Constable, London

Whitaker-Menezes, D., Martinez-Outschoorn, U. E., Lin, Z., Ertel, A., Flomenberg, N., Witkiewicz, A. K., … Lisanti, M. P. (2011). Evidence for a stromal-epithelial “lactate shuttle” in human tumors: MCT4 is a marker of oxidative stress in cancer-associated fibroblasts. Cell cycle (Georgetown, Tex.), 10(11), 1772–1783.

Wolf, A., Agnihotri, S., Munoz, D., & Guha, A. (2011). Developmental profile and regulation of the glycolysis enzyme hexokinase 2 in normal brain and glioblastoma multiforme. Neurobiology of disease, 44(1), 84–91. doi:10.1016/j.nbd.2011.06.007

World Health Organization. Women’s Health. Retrieved 6/15/2012 from http://www.who.int/mediacentre/factsheets/fs334/en/index.html. 2009

Xu, W., Zhou, J., Xie, Y., Wang, W., Zhao, Y., Chen, X., & Li, Y. (2012). [Association between the expression and methylation of energy-related genes with Helicobacter pylori infection in gastric cancer]. Zhonghua yi xue za zhi, 92(6), 366–370.

Yamashita, M., Ogawa, T., Zhang, X., Hanamura, N., Kashikura, Y., Takamura, M., … Shiraishi, T. (2012). Role of stromal myofibroblasts in invasive breast cancer: stromal expression of alpha-smooth muscle actin correlates with worse clinical outcome. Breast cancer (Tokyo, Japan), 19(2), 170–176. doi:10.1007/s12282-010-0234-5

Yazhou, C., Wenlv, S., Weidong, Z., & Licun, W. (2004). Clinicopathological significance of stromal myofibroblasts in invasive ductal carcinoma of the breast. Tumour biology: the journal of the International Society for Oncodevelopmental Biology and Medicine, 25(5-6), 290–295. doi:10.1159/000081394

Yeung, S. J., Pan, J., & Lee, M.-H. (2008). Roles of p53, MYC and HIF-1 in regulating glycolysis - the seventh hallmark of cancer. Cellular and molecular life sciences:

CMLS, 65(24), 3981–3999. doi:10.1007/s00018-008-8224-x

Zeisberg, E. M., Tarnavski, O., Zeisberg, M., Dorfman, A. L., McMullen, J. R., Gustafsson, E., … Kalluri, R. (2007). Endothelial-to-mesenchymal transition contributes to cardiac fibrosis. Nature medicine, 13(8), 952–961. doi:10.1038/nm1613